www.nature.com/aps

Acta Pharmacologica Sinica

ARTICLE

Caffeic acid alleviates cerebral ischemic injury in rats by resisting ferroptosis via Nrf2 signaling pathway

Xin-nan Li[1], Nian-ying Shang[1], Yu-ying Kang[1], Ning Sheng[1], Jia-qi Lan[1], Jing-shu Tang[1], Lei Wu[1], Jin-lan Zhang[1]✉ and Ying Peng[1]✉

There are few effective and safe neuroprotective agents for the treatment of ischemic stroke currently. Caffeic acid is a phenolic acid that widely exists in a number of plant species. Previous studies show that caffeic acid ameliorates brain injury in rats after cerebral ischemia/reperfusion. In this study we explored the protective mechanisms of caffeic acid against oxidative stress and ferroptosis in permanent cerebral ischemia. Ischemia stroke was induced on rats by permanent middle cerebral artery occlusion (pMCAO). Caffeic acid (0.4, 2, 10 $mg{\cdot}kg^{-1}{\cdot}d^{-1}$, i.g.) was administered to the rats for 3 consecutive days before or after the surgery. We showed that either pre-pMCAO or post-pMCAO administration of caffeic acid (2 $mg{\cdot}kg^{-1}{\cdot}d^{-1}$) effectively reduced the infarct volume and improved neurological outcome. The therapeutic time window could last to 2 h after pMCAO. We found that caffeic acid administration significantly reduced oxidative damage as well as neuroinflammation, and enhanced antioxidant capacity in pMCAO rat brain. We further demonstrated that caffeic acid down-regulated TFR1 and ACSL4, and up-regulated glutathione production through Nrf2 signaling pathway to resist ferroptosis in pMCAO rat brain and in oxygen glucose deprivation/reoxygenation (OGD/R)-treated SK-N-SH cells in vitro. Application of ML385, an Nrf2 inhibitor, blocked the neuroprotective effects of caffeic acid in both in vivo and in vitro models, evidenced by excessive accumulation of iron ions and inactivation of the ferroptosis defense system. In conclusion, caffeic acid inhibits oxidative stress-mediated neuronal death in pMCAO rat brain by regulating ferroptosis via Nrf2 signaling pathway. Caffeic acid might serve as a potential treatment to relieve brain injury after cerebral ischemia.

Keywords: ischemic stroke; caffeic acid; oxidative stress; neuroinflammation; ferroptosis; Nrf2

Acta Pharmacologica Sinica (2024) 45:248–267; https://doi.org/10.1038/s41401-023-01177-5

INTRODUCTION

Stroke is the second leading cause of death and the third leading cause of disability globally, and its impact is increasing rapidly in low-income and middle-income countries [1]. Ischemic stroke accounts for 80%–85% of all strokes [2]. Tissue-type plasminogen activator (tPA) is the only Food and Drug Administration-approved pharmacological therapy [3]. Oxidative stress caused by excessive production of reactive oxygen species in brain tissues is one of the key molecular mechanisms of stroke after restoration of blood flow (reperfusion) [4]. Several studies have shown increased biomarkers of oxidative stress in acute stroke patients [5, 6]. Of note, in vitro approaches and in vivo animal studies have also elucidated several ischemia-mediated biochemical and histological oxidative changes towards biomolecules, such as lipid peroxidation [2] and nucleic acid oxidation [7], as well as protein carbonylation [8] and nitrosylation [9]. Moreover, the therapeutic regimen for oxidative stress has been applied in clinical trials and has achieved effective results [10, 11].

Ferroptosis is a newly discovered form of cell death in acute brain injury, including cerebral ischemia and hemorrhage, marked by phospholipid oxidative modification of the membrane in an iron-dependent manner [12, 13]. Glutathione peroxidase 4 (GPX4) is a selenocysteine-containing protein that plays an important role in recovering phospholipid peroxide. Ferroptosis has been demonstrated to be initiated by GSH depletion or GPX4 activity inhibition [14]. *GPX4* expression is decreased during acute ischemia stroke [15]. Recent studies revealed that reducing iron accumulation and increasing the activity of the ferroptosis defence system might be an effective therapy for ischemic stroke. For example, treatment with iron chelators, such as deferoxamine mesylate (DFO), could prevent the production of free radicals and reduce serum levels of peroxides in stroke patients [16]. Interestingly, selenium supplementation effectively alleviated ferroptosis by alleviating *GPX4* expression after stroke [17]. Thus, the inhibition of ferroptosis might be essential for the treatment of ischemic stroke.

Nrf2 (NF-E2-related factor-2) is a member of the basic transcription factor family and plays important roles in the responses to antioxidant defences by binding to antioxidant response elements (AREs) of almost 200 antioxidant genes to increase their transcription, such as NAD(P)H quinone oxidoreductase 1 (NQO-1) and heme-oxygenase-1 (HO-1) [18–20]. Many studies have shown that the Nrf2 signaling pathway exerts important functions in both ischemia and ischemia/reoxygenation

[1]State Key Laboratory of Bioactive Substances and Functions of Natural Medicines, Institute of Materia Medica, Chinese Academy of Medical Sciences & Peking Union Medical College, Beijing 100050, China
Correspondence: Jin-lan Zhang (zhjl@imm.ac.cn) or Ying Peng (ypeng@imm.ac.cn)
These authors contributed equally: Xin-nan Li, Nian-ying Shang

Received: 12 May 2023 Accepted: 26 September 2023
Published online: 13 October 2023

events [21]. Animals with Nrf2 deletion were more likely to suffer from cerebral ischemic stroke with larger infarct sizes and more severe neurological deficits [22, 23]. The activation of the Nrf2 signaling pathway neutralizes ROS and mitigates the harmful effects of cerebral ischemia [24]. Moreover, Nrf2 signaling also regulates the cellular response to inflammation by suppressing proinflammatory genes and maintaining redox homeostasis [25]. Recent research demonstrated that hypersensitivity to LPS in Nrf2 knockout mice was higher than that in wild-type mice, and the levels of NO synthase, IL-6 and TNF-α in Nrf2 knockout mice were significantly increased [26]. In addition to antioxidant responses and inflammation defence, as an important regulator of lipid peroxidation, Nrf2 also regulates the expression of other protective genes, including ferroptosis genes such as GPX4, ferroportin (SLC40A1) and solute carrier family member 48 member A1 (SLC48A1) [27–29].

Dietary polyphenols, widely distributed in plant-derived foods, are beneficial to human health by exerting a variety of biological effects [30]. Caffeic acid, as a natural bioactive phenolic acid, has been explored due to its potential antioxidant properties [31]. Caffeic acid is rich in coffee, fruits and vegetables [32]. Moreover, caffeic acid has been found in multiple traditional Chinese medicines for ischemic stroke, such as Naoshuantong capsule, Dengzhan Xixin injection, and Dengzhanshengmai capsule [33–35]. Previous studies have reported that caffeic acid ameliorates brain injury in rats after cerebral ischemia/reperfusion [36], but the possible protective mechanisms of caffeic acid against oxidative stress and ferroptosis in permanent cerebral ischemia have not been reported. It is worth noting that only approximately 5% of ischemic stroke patients can receive thrombolytic therapy within a limited time window, and most stroke patients cannot achieve recanalization and reperfusion [37–40]. In summary, we demonstrated that caffeic acid significantly reduced ischemia induced cerebral injury. The main mechanism might be inhibiting oxidative stress-mediated neuronal death by regulating ferroptosis via the Nrf2 signaling pathway.

MATERIALS AND METHODS

Animals, permanent middle cerebral artery occlusion (pMCAO) ischemia model and drug treatments

Male Sprague–Dawley rats weighing 260–280 g were housed in plastic cages at 23 ± 1 °C. All rats were given adequate food and water and were kept on a 12 h light cycle. All experiments were approved and performed in accordance with the National Institute of Health Guidelines for the Care and Use of Laboratory Animals and approved by the institutional Ethics Committee of the Experimental Animal Center of the Chinese Academy of Medical Sciences (Beijing, China).

To simulate the clinical pathophysiological state of patients with ischemic stroke, a permanent middle cerebral artery occlusion (pMCAO) model was prepared [41–43]. The operation for permanent middle cerebral artery occlusion was previously described [44]. Specifically, rats were anaesthetized with isoflurane, and a midline incision was made in the neck. The lateral common carotid artery (CCA), external carotid artery (ECA) and internal carotid artery (ICA) were separated. The proximal CCA and distal ECA were ligated. The ECA was then incised, and a 4–0 silicon-coated monofilament suture (Φ0.26 mm, Beijing Cinontech Co., Ltd., Beijing, China) was inserted from the ECA to the ICA until the origin of the right middle cerebral artery was occluded. Sham-operated rats received the same surgical procedures without pMCAO. The pMCAO rats were randomly divided into four groups: the vehicle group and caffeic acid 0.4 mg/kg, 2 mg/kg and 10 mg/kg groups. Caffeic acid and control solvent were administered orally three consecutive days before surgery or after surgery. To further investigate the mechanism of action of caffeic acid, ML385 (i.v., 15 μg/kg) was administered intravenously before MCAO [45].

Measurement of cerebral infarction

Brain tissue samples were collected at 24 h or 3 d after ischemia stroke. Then, 2-mm-thick coronal sections were stained with 1% triphenyltetrazolium chloride (TTC) solution at 37 °C. The brain slices were turned over every 5 min for 40 min. The volume of cerebral infarction was measured as described above [46]. The infarct volume was calculated as a percentage according to following:

Infarct volume (%) = (area of contralateral hemisphere − area of noninfarcted region of ipsilateral hemisphere)/area of contralateral hemisphere × 100%

Neurological deficit assessment

Neurological deficits were assessed using the Bederson scoring system and the modified Neurological Severity Score (mNSS) test by an assessor blinded to the experimental groups. The Bederson scoring system evaluated forelimb flexion, resistance to lateral push and circling behavior, which was graded 0–4 according to the following criteria: 0, no neurological deficit; 1, flexion of contralateral forelimb; 2, severe forelimb flexion and decreased resistance to lateral push without circling; 3, unidirectional circling; and 4, loss of spontaneous motor activity and a depressed level of consciousness [47].

In addition, the mNSS test was performed on rats to assess their neurological functions, including motor, sensory, reflex and balance tests. The function is graded on a scale of 0 to 18 (normal score, 0; maximal deficit score, 18). Higher scores indicate more severe behavioral deficits [48].

Isolation and culture of rat primary microglia and primary neurons

To obtain a single primary neuron cell suspension, the brains of 24-h newborn rats were dissected and then digested with trypsin at 37 °C for 15 min. The cell suspension was then filtered through a 40 μm strainer. The isolated cells were subsequently cultured in DMEM supplemented with 1% penicillin–streptomycin solution and 10% fetal bovine serum at a concentration of 1×10^6 cells/ml. After 6 h, the medium was replaced with neurobasal culture medium (Gibco, USA) that consisted of 2% B27 and 100× glutamine and cultured for 10 days. The isolation method of primary microglia was similar to that of neurons. The cell suspension of mixed glial cells was cultured at 1×10^6 cells/ml for 14 days, and then primary microglia were purified by the manual collision method.

Cell culture and oxygen–glucose deprivation/reoxygenation (OGD/R) damage model of SK-N-SH cells and primary neurons

SK-N-SH cells, BV2 cells and primary microglia were cultured in DMEM supplemented with 1% penicillin–streptomycin liquid (Solarbio, P1400) and 10% fetal bovine serum (Yeasen, 40130ES76). Primary neurons were cultured in neurobasal culture medium (Gibco, USA) consisting of 2% B27, 0.5% penicillin–streptomycin liquid (Solarbio, P1400) and 100× glutamine (Beyotime Biotechnology, Shanghai, China). All cells were incubated in a humidified atmosphere with 5% CO_2 at 37 °C.

SK-N-SH cells were incubated with caffeic acid at different concentrations for 12 h and then transferred into low-glucose serum-free DMEM. After exposing the cells to hypoxia for 4 h, the low-glucose medium was replaced with normal medium for another 4 h. The treatment of primary neurons was similar to that of SK-N-SH cells, with both oxygen glucose deprivation and oxygen enrichment lasting for a period of 12 h.

LPS-induced proinflammatory damage model in BV2 cells

BV2 microglia were cultured in DMEM supplemented with 10% fetal bovine serum and 100 U/ml penicillin at 37 °C. The cells were

pretreated with DMEM supplemented with 2% fetal bovine serum and different concentrations of caffeic acid or DMSO for 6 h, followed by incubation with LPS (100 ng/ml, O55:B5, Sigma–Aldrich) or DMEM for 6 h.

Coculture of microglia and neurons

The coculture of neurons and microglia was achieved by using the Transwell system. Primary neurons were cultured at a concentration of 1×10^6 cells/ml in the lower compartment of the Transwell, while microglia were cultured at the same concentration in the upper compartment. A 0.4 μm semipermeable membrane separated the primary neurons and microglia, enabling the transmission of cell factors between the two compartments. After 10 ng/ml LPS stimulation of microglia, both microglia and neurons were incubated with caffeic acid at different concentrations and underwent oxygen-glucose deprivation (OGD) treatment for 20 h; indicators of inflammation and ferroptosis were then assessed.

Determination of catalase (CAT), glutathione peroxidase (GPx), glutathione (GSH), iron ion, malondialdehyde (MDA), nicotinamide adenine dinucleotide phosphate (NADPH), reactive oxygen species (ROS), superoxide dismutase (SOD), and total antioxidant capacity

The levels of CAT, GPx, NADPH, ROS, SOD and total antioxidant capacity were detected according to the manufacturer's instructions (Beyotime Biotechnology, Shanghai, China). Iron ion, GSH and MDA levels in cells were quantified as stated by the manufacturer (Nanjing Jiancheng Bioengineering Institute, Nanjing, China).

Determination of 8-hydroxy-2′-deoxyguanosine (8-OHdG)

The level of 8-OHdG was detected following the ELISA kit manufacturer's instructions (Cusabio, Wuhan, China). Then, 100 μL of standard or the supernatant of brain tissue homogenate was added per well and incubated for 2 h at 37 °C. Then, 100 μL of biotin-antibody was added to each well after removing the liquid and incubated for 1 h at 37 °C. Each well was aspirated and washed, and the process was repeated three times. Then, the steps were repeated using HRP-avidin before a total of five washes. Finally, 90 μL TMB substrate was added and incubated for 15 min at 37 °C, and 50 μL stop solution was added to stop the reaction. The optical density of each well was determined within 5 min by using a microplate reader at 450 nm.

Determination of protein carbonyl levels

Carbonylation of proteins was detected by protein carbonyl colorimetric assay. The supernatant of the brain tissue homogenate was transferred to a clean centrifuge tube, and streptomycin sulfate with a 10% volume fraction was added, fully mixed, and shaken intermittently at room temperature for 10 min. After centrifugation at $11{,}000 \times g$ for 5 min, 100 μL supernatant was added to 400 μL of 10 mmol/L DNPH (dissolved in 2 mol/L HCl). A blank control group was set, which was a 2 mol/L HCl solution without DNPH. Each reaction system was placed in the dark for 1 h and swirled once every 10 min. Then, 500 μL of 0.2 kg/L trichloroacetic acid (TCA) solution was added. Centrifugation was performed at 4 °C at $12{,}000 \times g$ for 15 min, and the supernatant was discarded. The precipitate was washed with 1 mL ethanol and ethyl acetate mixture ($v/v = 1{:}1$) 3 times, and the final precipitate was dissolved with 1.25 mL of 6 mol/L guanidine hydrochloride (37 °C for 15 min). After centrifugation at $12{,}000 \times g$ for 15 min, the absorbance value of the supernatant was measured at 370 nm.

Determination of TNF-α and IL-6 levels

The levels of TNF-α and IL-6 in the cell culture medium were measured with ELISA kits following the manufacturer's recommendations (BD Biosciences, USA; Invitrogen, USA).

NO assay

BV2 microglia were seeded into culture plates at a density of 2×10^5 cells/well. After 24 h, cells were pretreated with DMEM supplemented with 2% fetal bovine serum and different concentrations of caffeic acid or DMSO for 6 h and then incubated with or without LPS (100 ng/mL) for 6 h. An NO assay kit (Beyotime, Shanghai, China) was used to detect NO production in the cell supernatant.

MTT assay

10 μL of 5 mg/mL MTT solution was added to each well of the 96-well plate at 37 °C for 4 h. Then, the culture fluid was carefully removed from the well. Then, 150 μL of dimethyl sulfoxide was added, and the absorbance value of each well was measured at 570 nm.

DPPH assay

A DPPH· solution with a concentration of 1×10^{-4} mol/L was prepared with anhydrous ethanol. Then, 100 μL of DPPH· solution was added to the 96-well plate, followed by different concentrations of test sample solution and 100 μL of positive control vitamin C solution (the absorbance of this group was denoted as A1). At the same time, the DPPH· solution was replaced by 100 μL of anhydrous ethanol as a control to eliminate the interference of the color of the test sample itself on the test results (the absorbance of this group was denoted as A2). In addition, 100 μL anhydrous ethanol was used instead of the test sample (the absorbance of this group was denoted as A0). The 96-well plate was oscillated in a microplate reader for 1 min and stored at room temperature for 30 min under dark conditions. Then, the absorbance value was measured at 517 nm.

$$\text{DPPH} \cdot \text{clearance rate}(\%) = [\text{A0} - (\text{A1} - \text{A2})]/\text{A0} \times 100\%$$

Fenton reaction

30 μL of 0.75 mmol/L o-diphenanthrene solution was added to the 96-well plate. Then, 60 μL of PBS solution (pH 7.4) and 30 μL of distilled water were added. After fully mixing, 30 μL of 0.75 mmol/L ferrous sulfate solution and 30 μL of 1% H_2O_2 were added. Absorbance was measured at 536 nm after 60 min at 37 °C (the absorbance of this group was denoted as A0). H_2O_2 was replaced with 30 μL distilled water, and the above steps were repeated to determine the absorbance (the absorbance of this group was denoted as A1); 30 μL test solution was used instead of 30 μL distilled water to determine absorbance (the absorbance of this group was denoted as A2); only PBS solution and the test solution were added, and the other reagents were supplemented with distilled water. The above steps were repeated to measure the absorbance (the absorbance of this group was denoted as A3). PBS solution only was added, the other reagents were replaced with distilled water, and the above procedure was repeated to measure absorbance (the absorbance of this group was denoted as A4).

$$\text{OH clearance rate}(\%) = [(\text{A2} - \text{A3} - \text{A0} + \text{A4})/(\text{A1} - \text{A0})] \times 100\%$$

Oxygen radical absorbance capacity (ORAC) assay

Sample solution in the volume of 20 μL (vitamin C was selected as the positive control) was added to each well of the 96-well plate, then 20 μL of 75 mmol/L potassium phosphate buffer and 140 μL of 18.3 mmol/L AAPH were added, and finally 20 μL of 630 nmol/L sodium fluorescein was added to start the reaction. The 96-well plate was quickly placed in a fluorescence microplate reader to start the measurement at 37 °C, and a point was measured every 2 min until the fluorescence intensity was attenuated to a straight line. The antioxidant capacity of compounds could be reflected by comparing the protected integral area

netAUC on the fluorescence decay curve (the integral area under the fluorescence decay curve minus the area under the blank curve without antioxidant).

Pyrogallol autoxidation assay

A total of 180 μL of 0.05 mol/L Tris-HCl buffer solution (pH 8.2) was added to the 96-well plate, and then 40 μL of sample solution (vitamin C was selected as the positive control) and 16 μL of 9 mmol/L pyrogallol solution were added. Five minutes later, 8 μL of 3 mol/L HCl solution was added to terminate the reaction, and the absorbance was measured at 299 nm (the absorbance of this group was denoted as A1). In the model group, the sample solution was replaced with 40 μL of distilled water (the absorbance of this group was denoted as A0); in the reference solution control group, 40 μL of sample solution was added to 180 μL of 0.05 mol/L Tris-HCl buffer solution, and then 16 μL of distilled water was added after full mixing (the absorbance of this group was denoted as A1′). In the blank control group, pyrogallol and sample solution were replaced with 56 μL distilled water, and the above procedure was repeated to measure the absorbance (the absorbance of this group was denoted as A2).

$$O2^{-}\cdot \text{ clearance rate}(\%) = [A0 - (A1 - A1\prime) + A2]/A0] \times 100\%$$

Quantitative RT–PCR

RNA was extracted from rat brain tissues or cells with TRIzol reagent (TransGen Biotech, Cat ET111). After uniform quantification, RNA was reverse transcribed into cDNA using a Revert Aid First Strand cDNA Synthesis Kit (Yeasen, Cat 11141ES60). The sequences of primers used for qRT–PCR were as follows:

Nfe2l2: forward, 5′-GGTTGCCCACATTCCCAAAC-3′, reverse, 5′-TATCCAGGGCAAGCGACTCA-3′;

Hmox1: forward, 5′-CAGAAGAGGCTAAGACCGCC-3′, reverse, 5′-GCAGTATCTTGCACCAGGCTA-3′;

NQO-1: forward, 5′-CCATGTACGACAACGGTCCT-3′, reverse, 5′-GCAGGATGCCACTCTGAATC-3′;

Tnf-α: forward, 5′-CACGTCGTAGCAAACCACC-3′, reverse, 5′-GGTGAGGAGCACGTAGTCG-3′;

Il-1b: forward, 5′-TGCCACCTTTTGACAGTGATG-3′, reverse, 5′-TGATGTGCTGCTGCGAGATT-3′;

IL-6: forward, 5′-CCTCTCTGCAAGAGACTTCCAT-3′, reverse, 5′-ACAGGTCTGTTGGGAGTGGT-3′;

NOS2: forward, 5′-GGTGAAGGGACTGAGCTGTT-3′, reverse, 5′-ACGTTCTCCGTTCTCTTGCAG-3′.

β-actin: forward, 5′-CGCAGCCACTGTCGAGTC-3′, reverse, 5′-GTCATCCATGGCGAACTGGT-3′.

Western blotting

Protein samples from operative hemispheres of rats or cells were prepared using RIPA lysis buffer supplemented with complete EDTA-free protease inhibitor mixtures (Roche, Indianapolis, IN) and phosphatase inhibitor mixtures (Roche, Indianapolis, IN). Protein samples were separated on SDS-polyacrylamide gels and transferred to PVDF membranes. The membrane was blocked with 5% nonfat milk for 2 h and subsequently incubated with the following primary antibodies overnight at 4 °C: Nrf2 (16396-1-AP, 1:2000), GCLC (12601-1-AP, 1:2000), GCLM (14241-1-AP,1:2000), GFAP (16825-1-AP, 1:2000), COX2 (66351-1-Ig, 1:2000), iNOS (18985-1-AP, 1;2000), GAPDH (60004-1-Ig, 1:5000), p-AKT (66444-1-AP, 1:1000), AKT (10176-2-AP, 1:1000), SLC7A11 (26864-1-AP, 1:2000) and GSK3β (22104-1-AP, 1:1000) from Proteintech (Rosemont, IL,USA); GSR (sc-133245, 1:500), GSS (sc-166882, 1:500), 5-LOX (sc-136195) and SLC3A2(sc-390154, 1:500) from Santa Cruz Biotechnology (Dallas, TX, USA); HO-1 (ab68477, 1:2000), NQO-1 (ab80588, 1:1000), GPX4 (ab125066, 1:2000), ACSL4 (ab155282, 1:2000) and TFR1 (ab269513, 1:2000) from Abcam (Cambridge, UK); p-GSK3β (9SS6S, 1:1000) from Cell Signaling Technology (Danvers, MA, USA); β-Actin (TA-09, 1:2000) from ZSGBBIO (Beijing, China). Then, anti-mouse or anti-rabbit IgG-HRP (1:2000, ZSGB-BIO, ZB-2301; ZB-2305) was used, and the protein signals were detected.

Immunofluorescence staining

The brain tissue sections of rats were deparaffinized, rehydrated and then antigen repaired with Tris-EDTA antigen repair solution. After blocking nonspecific binding, the primary antibody anti-GFAP (1:400, M0761, Dako, Copenhagen, Denmark) was used at 4 °C. Then, Alexa Fluor Plus 488-conjugated secondary antibodies (1:200, A32731, Thermo Fisher Scientific) were added for 1 h at room temperature. The images were examined by a fluorescence microscope (PerkinElmer, USA) and analyzed using ImageJ 8.0 software.

Nissl staining

The brain sections of rats were dewaxed with a dewaxing agent and then immersed in different concentrations of ethanol. After dewaxing, coronal sections of rat brain tissue were immersed in Nissl staining solution (Beyotime Biotechnology, Shanghai, China), which was washed off after 30 min. The brain sections were then sealed with neutral balsam and further photographed under a microscope.

RNA-seq

Total RNA was extracted from rat brain tissue, and the constructed cDNA library was sequenced using BGIseq 500 (BGI-Shenzhen, China). We used HISAT2 (v2.0.4) to locate these reads to the Ensembl rat (mRatBN7.2) reference genome. DESeq2 (v1.4.5) with a Q value less than 0.05 was used for differential expression analysis.

Statistical analysis

All data are presented as the mean ± SEM using GraphPad Prism 8.0.1 software. Two-tailed unpaired Student's t tests was used to determine statistical significance. Differences at $P < 0.05$ were considered statistically significant.

RESULTS

Caffeic acid scavenged free radicals in vitro

The antioxidant capacity of caffeic acid, a natural phenolic acid, to scavenge free radicals was investigated. The DPPH assay is one of the most widely used methods to explore the free radical scavenging ability of compounds. Caffeic acid had a higher scavenging ability for DPPH free radicals than vitamin C at all four doses (Supplementary Fig. S1a). Similar findings could be seen in the oxidative radical and ·OH scavenging ability of caffeic acid (Supplementary Fig. S1b–d). In summary, the scavenging assay showed that caffeic acid had a stronger scavenging ability for DPPH·, ·OH and oxidative radicals than vitamin C. However, the intensity of vitamin C scavenging O2·- was stronger than that of caffeic acid (Supplementary Fig. S1e). These results suggested that caffeic acid could directly scavenge a variety of free radicals, further showing an excellent antioxidant effect in vitro.

Caffeic acid reduced ischemic brain injury in pMCAO rats

To further investigate the protective effect of caffeic acid on ischemia stroke, the cerebral infarction volume and nerve function of the pMCAO rat model at 24 h after the operation were studied by pretreatment. Three different doses of caffeic acid were given orally continuously 3 d before the MCAO operation (Supplementary Fig. S2a). Caffeic acid showed the best neuroprotective effects at a dose of 2 mg/kg, significantly reducing infarct volume and improving neurobehavioural scores (Supplementary Fig. S2b–e). To better represent the actual clinical situation, we extended the

duration of cerebral ischemia and used postoperative administration (Fig. 1a). Similar neuroprotective effects were found. Specifically, 2 mg/kg caffeic acid also reversed nerve damage caused by cerebral ischemia (Fig. 1b–e). Moreover, as determined by Nissl staining, the number of neurons in the peri-infarct region of caffeic acid-treated rats was also increased (Supplementary Fig. S3a, b). Then, we administered caffeic acid at 5 min, 0.5 h, 1 h, 2 h, and 3 h after MCAO surgery to explore the therapeutic time window. The experimental results showed that the protective effect of caffeic acid could last up to 2 h after pMCAO (Supplementary Fig. S4a–d). MDA, 8-OHdG and PC have been extensively studied as classical markers of oxidative damage to lipids, DNA and proteins. The improvement effect of caffeic acid on lipid and DNA oxidation was stronger than that on protein oxidation after cerebral ischemia (Fig. 1f–h). In addition, caffeic acid resulted in a significant increase in GPx and SOD (Fig. 1j–k) and slightly reversed the downregulation of total antioxidant capacity (Fig. 1i). Taken together, caffeic acid exerted a neuroprotective function by reducing oxidative stress damage in cerebral ischemic rats.

Caffeic acid protected SK-N-SH cells from OGD/R-induced oxidative stress

The neuroprotective effects of caffeic acid on ischemia stroke were further confirmed in an OGD/R cell injury model. Caffeic acid exhibited a concentration-dependent protective effect on OGD/R-injured neuronal cells (Supplementary Fig. S5a). Then, several oxidative stress damage markers and antioxidant capacity were detected to confirm the antioxidant capacity of caffeic acid in vitro. Compared with the model group, the levels of MDA and ROS were significantly decreased after caffeic acid treatment (Supplementary Fig. S5b, c). Total antioxidant capacity was significantly reduced after OGD/R damage; however, caffeic acid reversed this change (Supplementary Fig. S5d). The content of NADPH was significantly increased at 30 μmol/L caffeic acid (Supplementary Fig. S5e). Apart from the above antioxidant substances, caffeic acid also increased GPx activity relative to the model group (Supplementary Fig. S5f). However, the activity of CAT decreased in a dose-dependent manner with increasing caffeic acid concentration, which might be due to a compensatory effect (Supplementary Fig. S5g). Moreover, there were no changes in SOD activity in our OGD/R-damaged cell model (Supplementary Fig. S5h). Together, these results indicated that caffeic acid might be effective in reversing OGD/R-induced oxidative stress.

Caffeic acid exerted neuroprotective effects via the Nrf2 signaling pathway

To further explore the mechanism of the protective effect of caffeic acid on cerebral ischemia, RNA-seq was used to further analyze the brain tissues of MCAO rats (Fig. 2a). Notably, administration of caffeic acid improved DNA-binding transcription factor activity (Fig. 2b). In addition, gene enrichment analysis (GSEA) indicated that caffeic acid mainly increased the gene expression of antioxidant-related and anti-inflammatory-related pathways, including flavin adenine dinucleotide binding, guanylate cyclase activity, oxygen carrier activity, and ATPase activity (Fig. 2c). Nrf2 is well known as a key transcription factor of the antioxidant response that regulates downstream target gene expression. Considering the important cellular protective effect of Nrf2, we conducted a detailed study on the Nrf2 signaling pathway. Compared with the pMCAO model group, caffeic acid increased the mRNA levels of *Nfe2l2*, *Hmox1* and *Nqo1* at a 2 mg/kg dose (Fig. 3a–c) and obviously increased the protein expression of Nrf2 and its downstream genes, including HO-1, NQO-1, GCLC and GCLM, at a dose of 2 mg/kg after pMCAO treatment (Fig. 3f–i). Next, we tried to determine the upstream proteins of Nrf2. The phosphorylation levels of AKT and GSK3β were detected by Western blotting. As shown in Fig. 3d, e, the pMCAO model group had significantly decreased phosphorylation levels of AKT and GSK3β compared with the sham group. Caffeic acid markedly reversed the decreased phosphorylation levels of AKT and GSK3β. These results suggested that caffeic acid might reverse pMCAO-induced injury through the Nrf2 pathway in vivo.

Similarly, the Western blotting results in the OGD/R neuronal cell damage model showed that caffeic acid also upregulated Nrf2, HO-1 and NQO-1 expression in vitro (Fig. 4a–d). ML385, a Nrf2 inhibitor, could directly interact with the Nrf2 protein. The addition of 5 μmol/L ML385 reduced the expression of Nrf2, HO-1 and NQO-1 in cells despite the addition of caffeic acid (Fig. 4e–h). Then, we clearly found that the protective effect of caffeic acid on OGD/R damage was inhibited along with the inhibition of the Nrf2 signaling pathway, which was specifically manifested in the decrease in the cell survival rate, the increase in MDA content, the decrease in total antioxidant capacity and the decrease in GPx activity (Fig. 4i–l). Overall, caffeic acid exerted a neuroprotective function via the Nrf2 signaling pathway.

Caffeic acid reversed ferroptosis via the Nrf2 signaling pathway

Ferroptosis is a newly discovered type of iron-dependent programmed cell death that is regulated by lipid peroxidation and GPX4 [49]. The above study demonstrated that caffeic acid robustly relieved lipid peroxidation and elevated GPx activity in cerebral ischemia models. Here, our study found that brain iron ion levels in the pMCAO model rats were significantly increased compared to those in the sham operation group. Caffeic acid reversed the increase in iron ions in the pMCAO rat brain (Fig. 5a). GSH, as an important intracellular antioxidant, can clear lipid peroxides through glutathione peroxidase. Compared with the model group, the content of GSH in the brain tissue of rats was significantly upregulated after caffeic acid treatment (Fig. 5b). In addition, caffeic acid increased the expression levels of GSS and GSR, which are conducive to the further synthesis of GSH (Fig. 5c–e). Current studies have shown that downregulated GPX4 expression in cells makes them more sensitive to iron death and that upregulated GPX4 expression leads to a tolerance to iron death. Accordingly, we first explored the change in GPX4 expression after caffeic acid treatment. The results showed that GPX4 levels in rat brain tissue were significantly decreased after pMCAO operation. Moreover, caffeic acid upregulated the expression level of GPX4 (Fig. 5f, j), suggesting that caffeic acid plays a role in resistance to ferroptosis. SLC3A2, as one of the essential subunits in the GSH synthesis pathway, is also of great interest. We found that caffeic acid reversed the decline in SLC3A2 in the brains of pMCAO rats, suggesting that caffeic acid exerted a neuroprotective function by enhancing the GSH synthesis pathway (Fig. 5g, k). ACSL4, as an important isozyme, is essential for polyunsaturated fatty acid (PUFA) metabolism. Recent studies have shown that high ACSL4 expression makes cells more sensitive to ferroptosis by preferentially catalyzing several PUFAs, such as arachidonic acid (AA), and shaping the cellular lipid composition [50]. Notably, the level of ACSL4 in the brain tissue of pMCAO rats tended to be consistent with that of the sham group after caffeic acid treatment (Fig. 5h, l). Transferrin receptor 1 (TFR1) is an important membrane protein for the uptake of iron by cells and a limiting step for the entry of iron into cells, which is crucial to prevent cellular iron overload. Similarly, compared with the pMCAO model group, caffeic acid decreased TFR1 expression in rats (Fig. 5i, m). Next, we further explored the protective effect of caffeic acid on ferroptosis by using an OGD/R cell damage model. Elevated levels of iron ions and decreased levels of GSH were found in the cells after OGD/R (Fig. 6a, b). As expected, we detected similar in vitro changes in the expression of GPX4, SLC3A2, ACSL4 and TFR1 in the constructed OGD/R cell damage model, which proved the occurrence of ferroptosis in the cell model (Fig. 6c–j). It should be noted that caffeic acid also protects against ferroptosis by these measures in vitro. Then, we further

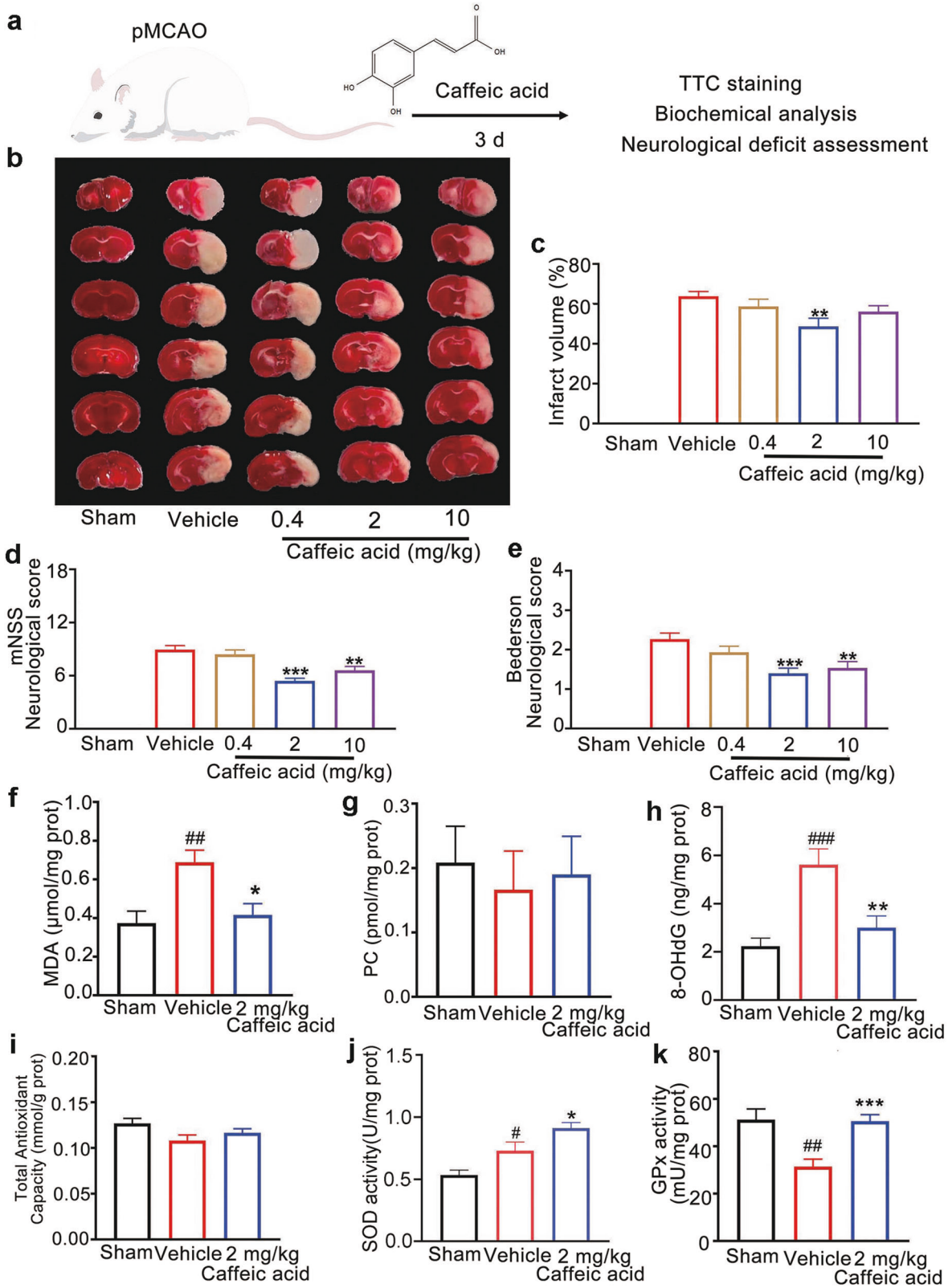

Fig. 1 Effects of caffeic acid on cerebral infarction volume, neurobehavioural scores, antioxidant enzymes and oxidative damage indices in pMCAO rats. a Experimental design process. **b**, **c** Cerebral infarction volume of pMCAO rats. **d** mNSS Neurobehavioural scores of pMCAO rats. **e** Bederson Neurobehavioural scores of pMCAO rats (sham group: $n = 3$, vehicle and caffeic acid group: $n = 15$). **f** The levels of MDA in pMCAO rat brains ($n = 5$). **g** The levels of protein carbonylation in pMCAO rat brains ($n = 5$). **h** The level of 8-OHdG in pMCAO rat brains ($n = 8$). **i** The level of total antioxidant capacity in pMCAO rat brains ($n = 10$). **j** The activities of SOD in pMCAO rat brains ($n = 13$). **k** The activities of GSH-Px in pMCAO rat brains ($n = 10$). Data are shown as the mean ± SEM, $^{\#}P < 0.05$, $^{\#\#}P < 0.01$, $^{\#\#\#}P < 0.001$ vs. the sham group, $^{*}P < 0.05$, $^{**}P < 0.01$ and $^{***}P < 0.001$ vs. the vehicle group.

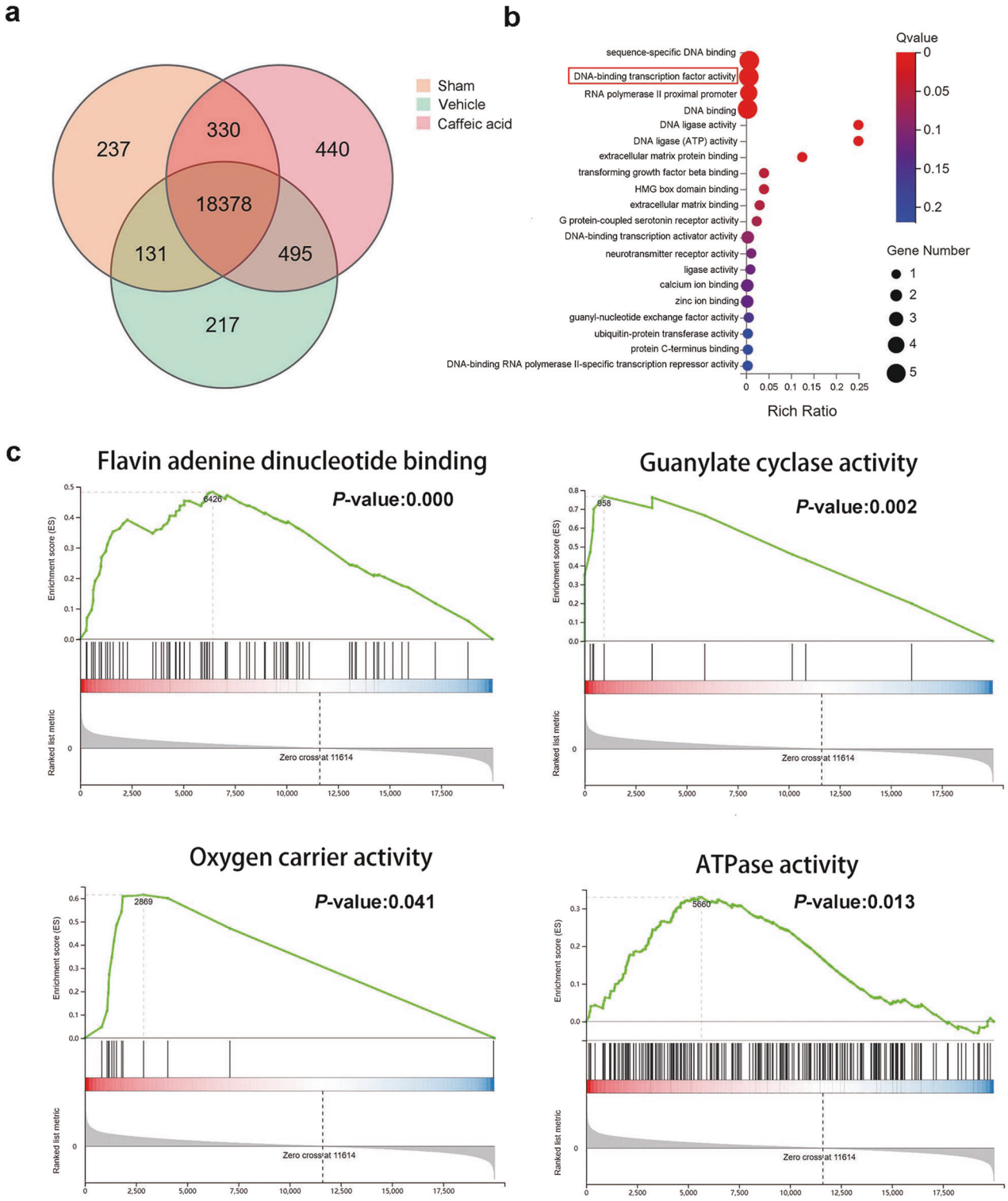

Fig. 2 RNA-seq analysis of genes in pMCAO rat brain tissues. a Genes in the sham group, vehicle group and caffeic acid group. **b** GO molecular function analysis in the vehicle group vs. the caffeic acid group. **c** Gene enrichment analysis (GSEA) indicated antioxidant- and anti-inflammation-related pathways, including flavin adenine dinucleotide binding, guanylate cyclase activity, oxygen carrier activity, and ATPase activity. (sham group: $n = 3$, vehicle group: $n = 3$ and caffeic acid group: $n = 5$).

explored the association between Nrf2 and ferroptosis. When ML385 was added, the effect of caffeic acid on iron ion reduction and GSH increase was inhibited (Fig. 7a, b). In addition, the levels of GPX4, ACSL4 and TFR1 became identical to those in the model group after the Nrf2 signaling pathway was suppressed (Fig. 7c–g). We found similar results in vivo, and ML385 reversed the improvement in cerebral ischemia induced by caffeic acid in pMCAO rats (Fig. 8a–d). At the same time, the regulation of caffeic acid on iron ions and GSH was also inhibited by ML385 (Fig. 8e, f). WB results also showed that ML385 treatment reversed caffeic

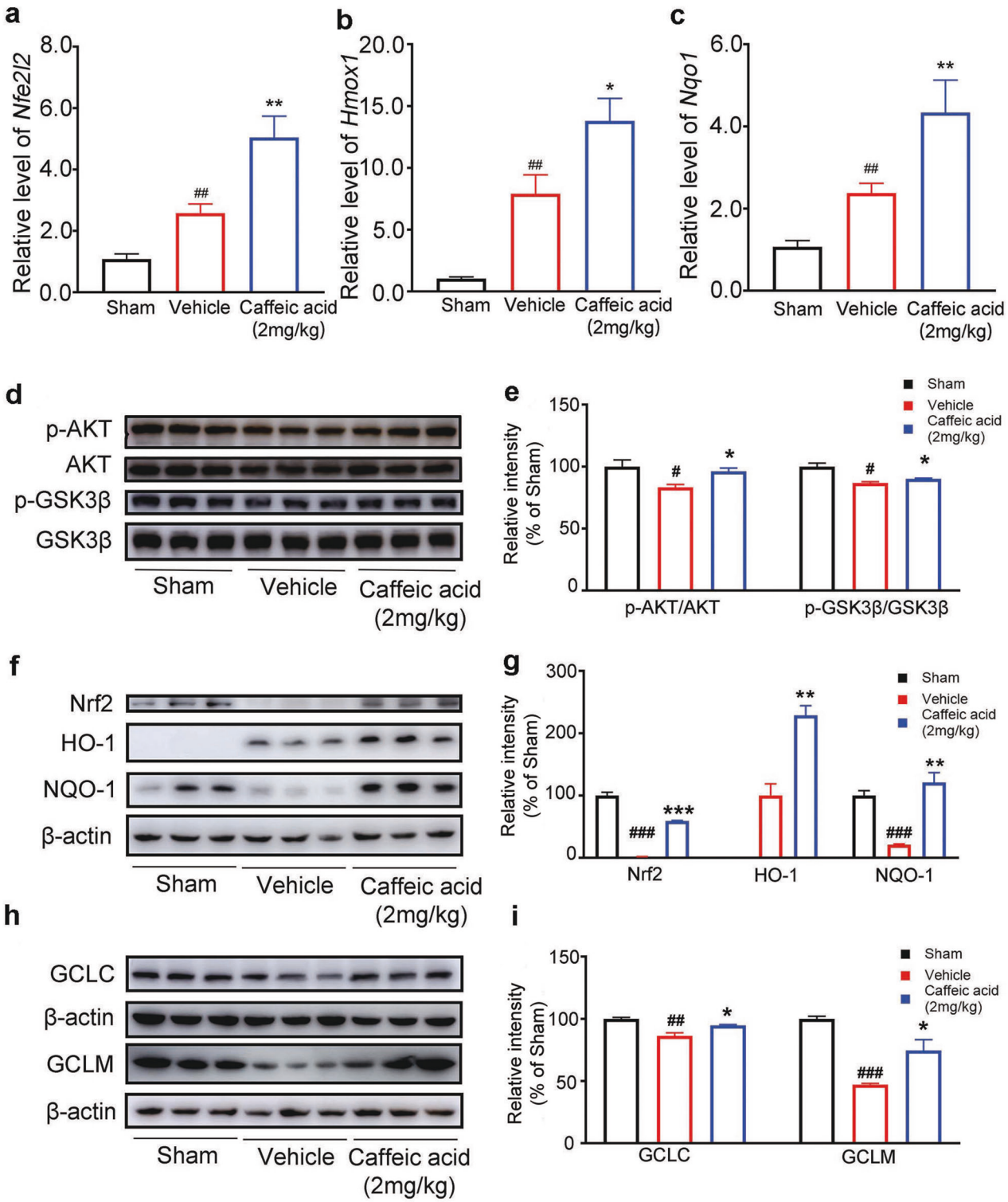

Fig. 3 Caffeic acid upregulates the Nrf2 signaling pathway after cerebral ischemia. a–c The mRNA transcription of the Nrf2 pathway in the brain tissue of pMCAO rats ($n = 6–9$). **d**, **e** Representative WB bands and the relative changes in p-AKT/AKT and p-GSK3β/GSK3β protein levels after caffeic acid treatment in pMCAO rats ($n = 3$). **f**, **g** Representative WB bands and the relative changes in Nrf2, HO-1, and NQO-1 protein levels after caffeic acid treatment in pMCAO rats ($n = 3$). **h**, **i** Representative WB bands and the relative changes in GCLC and GCLM protein levels after caffeic acid treatment in pMCAO rats ($n = 3$). Data are shown as the mean ± SEM, $^{\#}P < 0.05$, $^{\#\#}P < 0.01$ and $^{\#\#\#}P < 0.001$ vs. the sham group, $^{*}P < 0.05$, $^{**}P < 0.01$ and $^{***}P < 0.001$ vs. the vehicle group.

acid-induced protein expression changes in ACSL4, TFR1, SLC7A11 and GPX4 in pMCAO rats (Fig. 8g–j). In summary, these results suggested that caffeic acid further inhibited ferroptosis after cerebral ischemia through the Nrf2 signaling pathway.

Caffeic acid suppressed neuroinflammation and resisted ferroptosis in vitro and in vivo

Active astrocytes and microglia are found in the poststroke pathological process. The surge in ROS after stroke promotes the

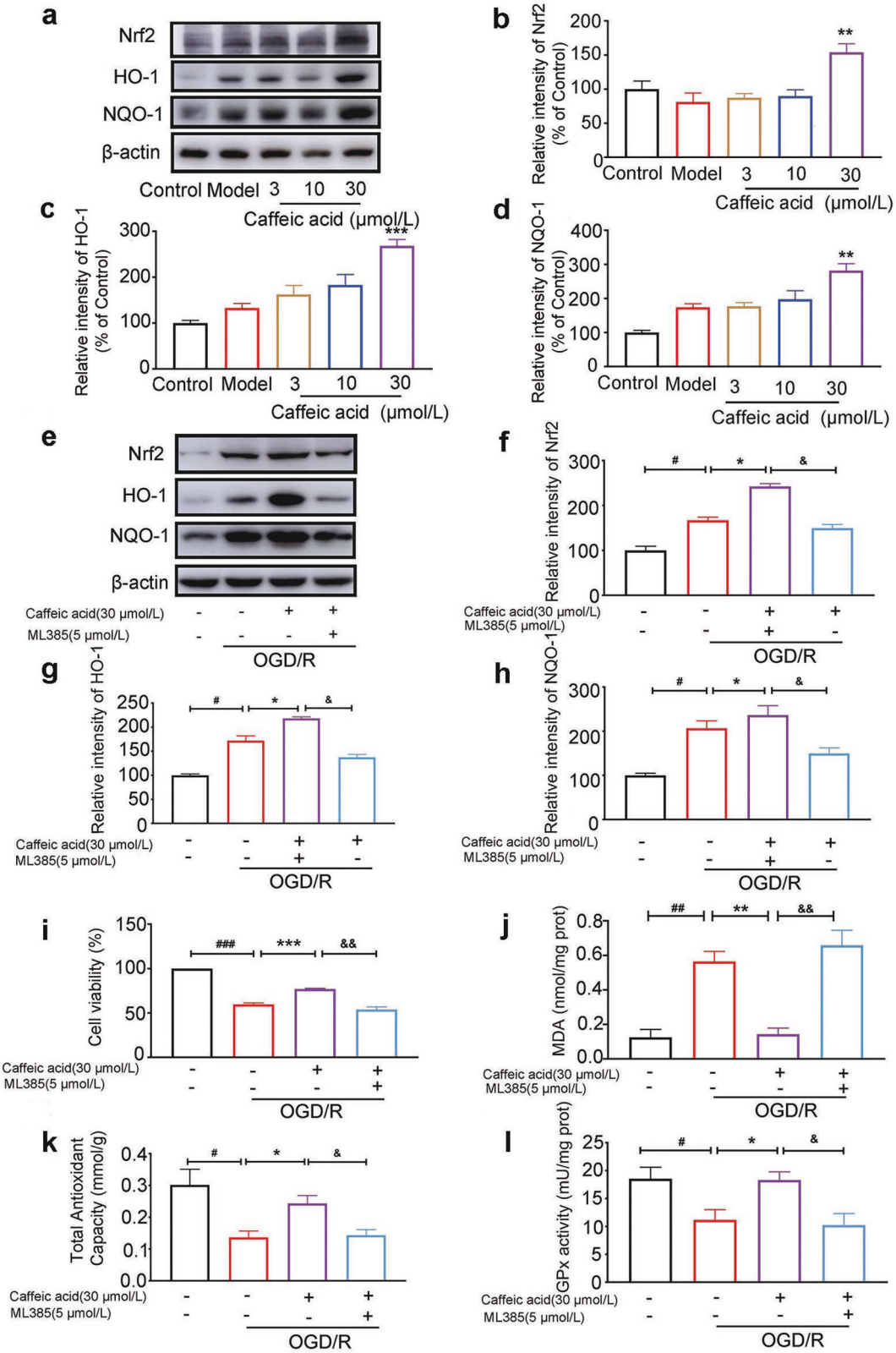

Fig. 4 Caffeic acid exerted neuroprotective effects via the Nrf2 signaling pathway in OGD/R-treated SK-N-SH cells. a–d Representative WB bands and quantitative analysis of Nrf2, HO-1 and NQO-1 in the OGD/R-treated SK-N-SH cell model after caffeic acid treatment ($n = 3$). **e–h** The effects of ML385 on the expression of Nrf2, HO-1, and NQO-1 ($n = 3$). **i** Cell viability was measured by MTT assay ($n = 3$). **j** MDA levels in OGD/R-damaged SK-N-SH cells treated with caffeic acid or ML385 ($n = 3$). **k** The level of total antioxidant capacity in OGD/R-damaged SK-N-SH cells treated with caffeic acid or ML385 ($n = 3$). **l** The level of GPx activity in OGD/R-damaged SK-N-SH cells treated with caffeic acid or ML385 ($n = 4$). The Western blot is representative of three independent experiments. Data are shown as the mean ± SEM, $^{\#}P < 0.05$, $^{\#\#}P < 0.01$ and $^{\#\#\#}P < 0.001$ vs. the control group, $^{*}P < 0.05$, $^{**}P < 0.01$ and $^{***}P < 0.001$ vs. the model group, $^{\&}P < 0.05$ and $^{\&\&}P < 0.01$ vs. the caffeic acid group.

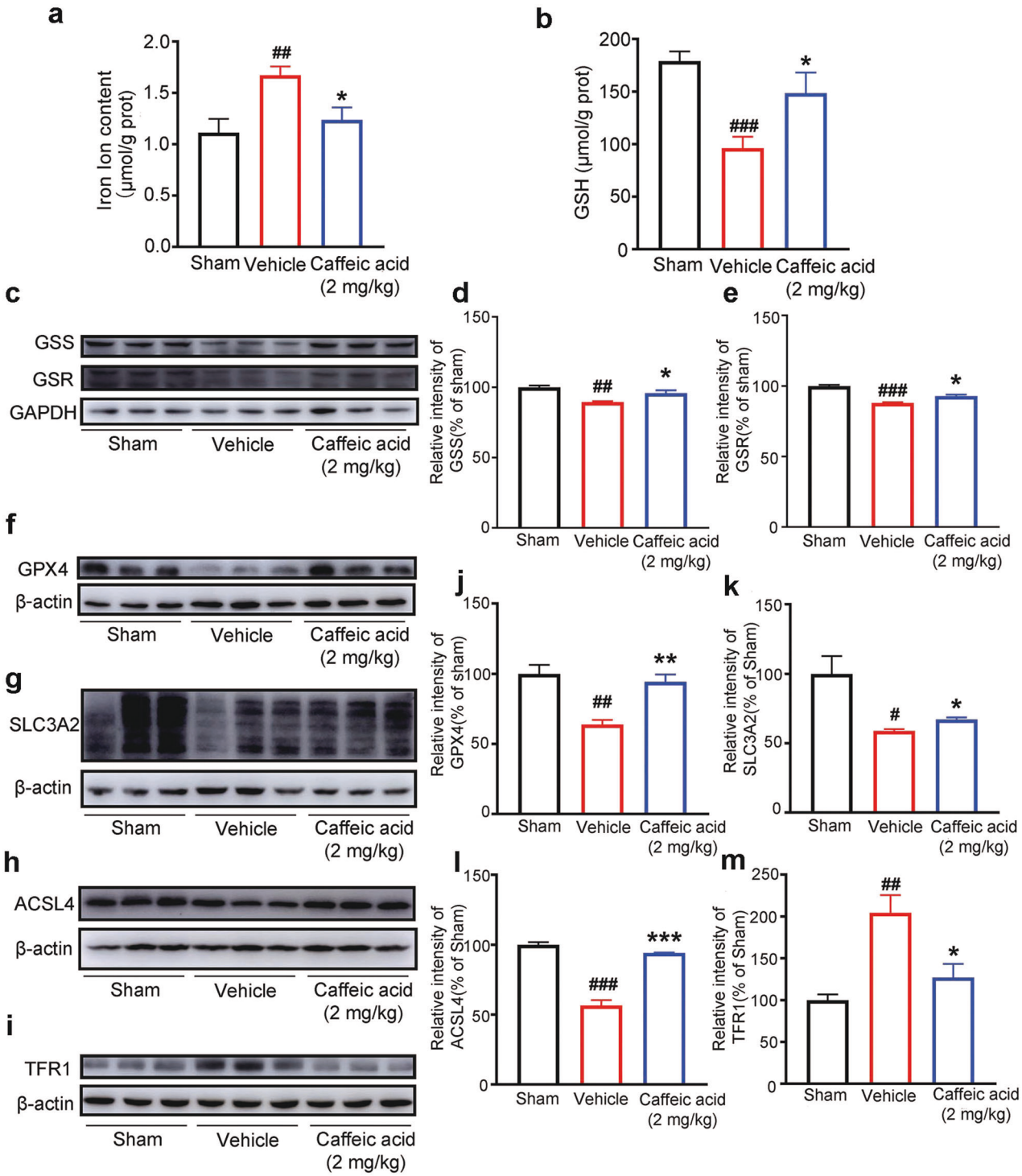

Fig. 5 Caffeic acid inhibited ferroptosis in pMCAO rats. a The protective effect of caffeic acid on intracellular iron content in pMCAO rats. ($n = 5$). **b** The improving effect of caffeic acid on GSH content in pMCAO rats ($n = 5$). **c**–**e** The effects of caffeic acid on GSS and GSR protein levels ($n = 3$). **f**, **j** The effects of caffeic acid on GPX4 protein levels ($n = 3$). **g**, **k** The effects of caffeic acid on SLC3A2 protein levels ($n = 3$). **h**, **l** The effects of caffeic acid on ACSL4 protein levels ($n = 3$). **i**, **m** The effects of caffeic acid on TFR1 protein levels ($n = 3$). The Western blot is representative of three independent experiments. Data are shown as the mean ± SEM, $^{\#}P < 0.05$, $^{\#\#}P < 0.01$, $^{\#\#\#}P < 0.001$ vs. the sham group, $^{*}P < 0.05$, $^{**}P < 0.01$ and $^{***}P < 0.001$ vs. the vehicle group.

release of multiple proinflammatory mediators from microglia [51]. First, the anti-inflammatory activity of caffeic acid in vivo was detected. Surprisingly, caffeic acid markedly reduced the protein levels of COX2 and GFAP in the brain tissue of pMCAO rats (Fig. 9a, b). Then, the accumulation and activation of astrocytes were detected. The immunofluorescence results showed that activated astrocytes intensely accumulated in the peri-infarct (penumbra) region 3 days after the pMCAO operation. It is worth noting that caffeic acid significantly reduced the density of astrocytes and restored the

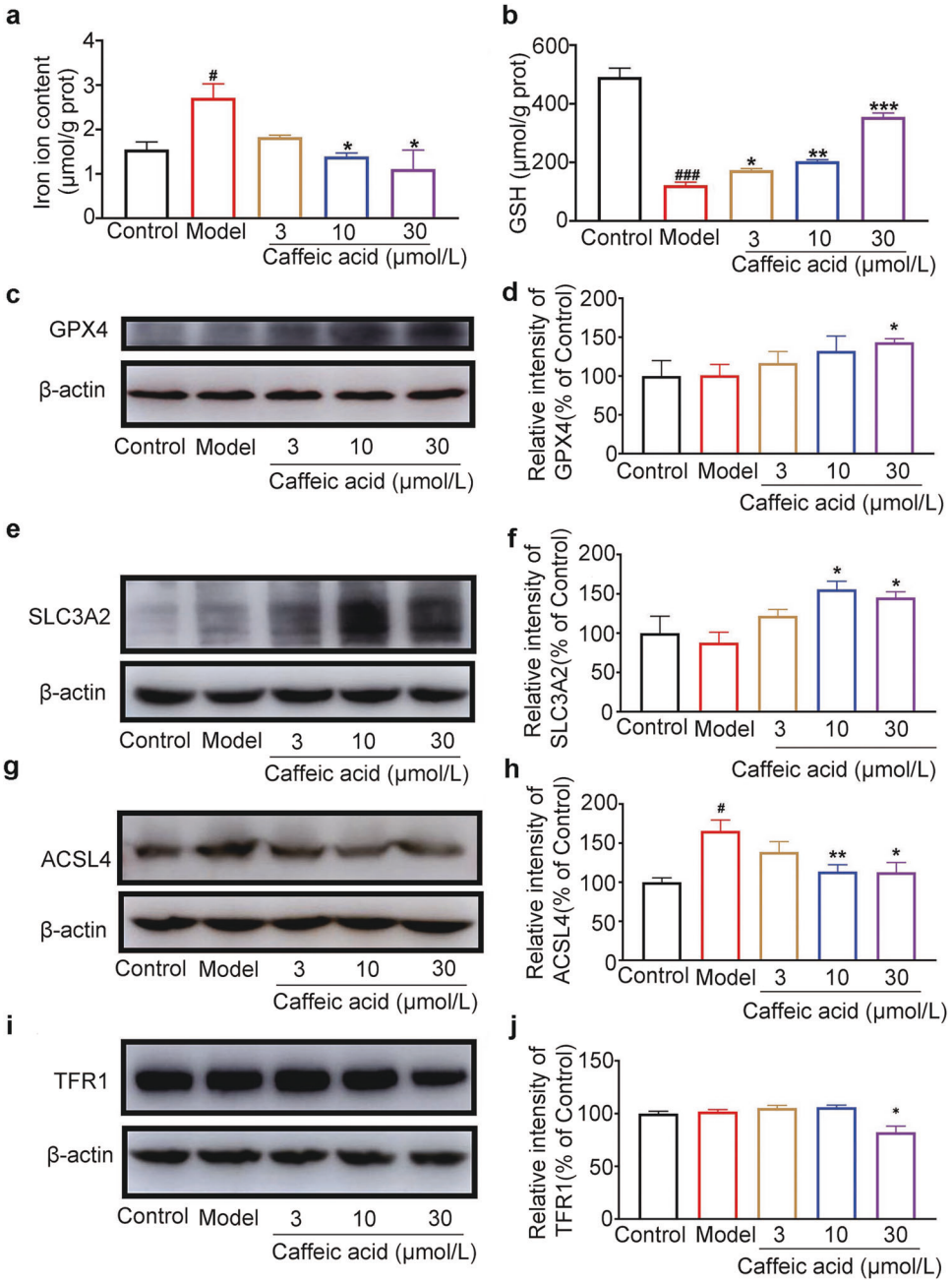

Fig. 6 Caffeic acid inhibited ferroptosis in OGD/R-damaged cells. a The protective effect of caffeic acid on intracellular iron content in OGD/R-treated SK-N-SH cells. ($n = 3$). **b** The improving effect of caffeic acid on GSH content in OGD/R-treated SK-N-SH cells ($n = 3$). **c**, **d** The effect of caffeic acid on GPX4 protein levels ($n = 3$). **e**, **f** The effect of caffeic acid on SLC3A2 protein levels ($n = 3$). **g**, **h** The effect of caffeic acid on ACSL4 protein levels ($n = 3$). **i**, **j** The effect of caffeic acid on TFR1 protein levels ($n = 3$). The Western blot is representative of three independent experiments. Data are shown as the mean ± SEM, $^{\#}P < 0.05$ and $^{\#\#\#}P < 0.001$ vs. the control group, $^{*}P < 0.05$, $^{**}P < 0.01$ and $^{***}P < 0.001$ vs. the model group.

morphological alterations resulting from pMCAO (Fig. 9c, d). These data suggested that caffeic acid exerted an anti-inflammatory effect on ischemic stroke in pMCAO rats.

The MTT assay results showed that all doses of caffeic acid had no effect on the viability of BV2 cells with or without 100 ng/mL LPS treatment (Supplementary Fig. S6a). Then, the effects of caffeic acid on proinflammatory cytokines and mediators were detected. The results of ELISA and Griess assays showed that caffeic acid inhibited proinflammatory cytokine (IL-6 and TNF-α) release and NO production in BV2 microglia (Fig. 10a–c). Moreover, the mRNA levels of proinflammatory genes were determined by qRT–PCR. Caffeic acid significantly reduced the mRNA levels of *TNF-α*, *IL-6*, *IL-1β* and *NOS2* (Fig. 10d–g). The inhibitory effect of caffeic acid on iNOS expression was then confirmed by Western blot analysis (Fig. 10k–l). The above results indicated that caffeic acid can inhibit the inflammatory response and further play an effective anti-inflammatory role. Next, downstream proteins of the Nrf2 signaling pathway were also detected. Caffeic acid induced HO-1 and NQO-1 expression at the mRNA and protein levels (Fig. 10h–j, m–q). Thus, the results demonstrated that caffeic acid might suppress the proinflammatory response via Nrf2 signaling.

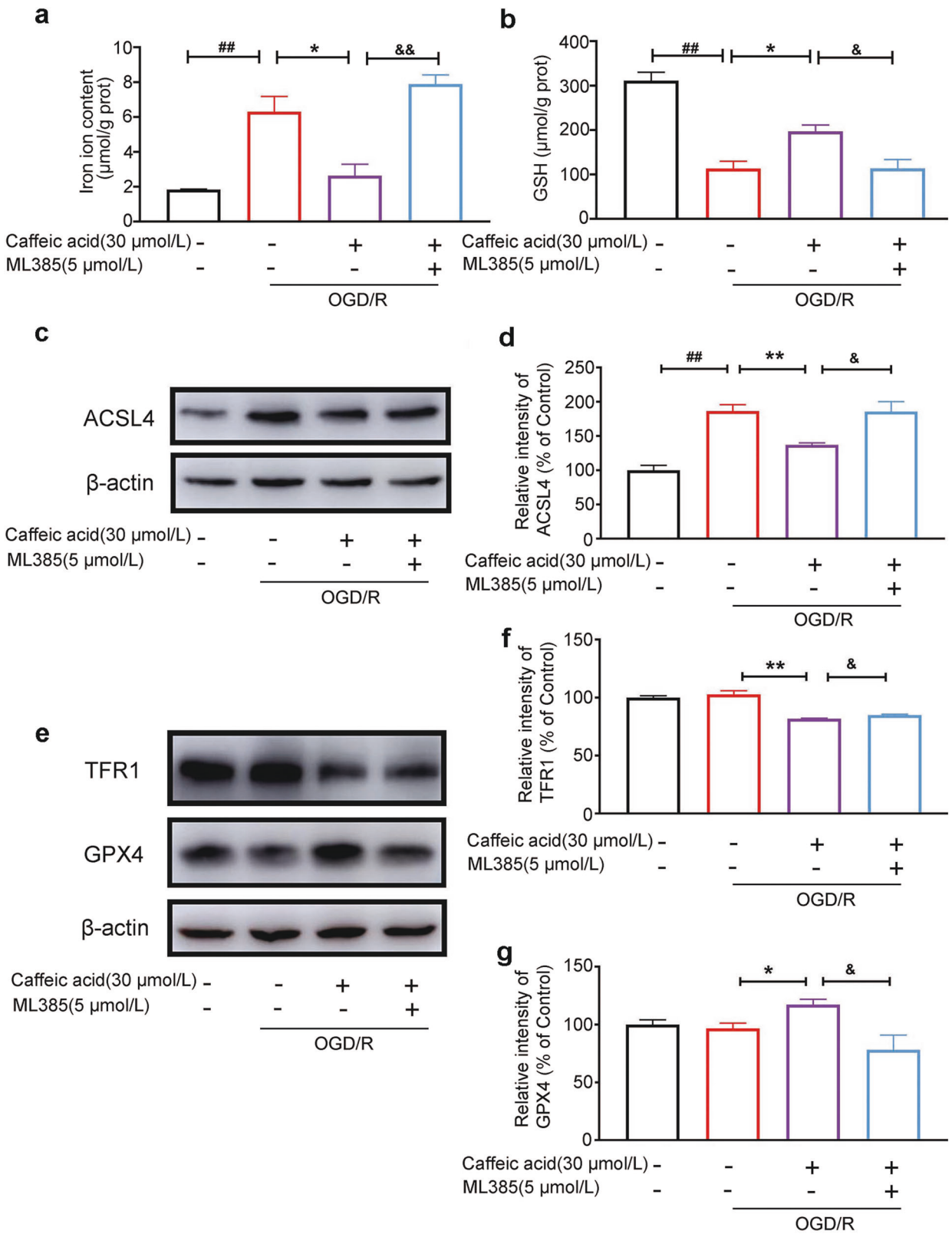

Fig. 7 Caffeic acid reversed ferroptosis via the Nrf2 signaling pathway in vitro. ML385, an inhibitor of Nrf2, reversed the protective effect of caffeic acid on intracellular iron content (**a**) and GSH content (**b**) in OGD/R-treated SK-N-SH cells ($n = 3$). The expression of ACSL4 (**c**, **d**), TFR1 (**e**, **f**) and GPX4 (**e**, **g**) was measured by Western blotting. The Western blot is representative of three independent experiments ($n = 3$). Data are shown as the mean ± SEM, $^{\#\#}P < 0.01$ vs. the control group, $^{*}P < 0.05$ and $^{**}P < 0.01$ vs. the model group, $^{\&}P < 0.05$ and $^{\&\&}P < 0.01$ vs. the caffeic acid group.

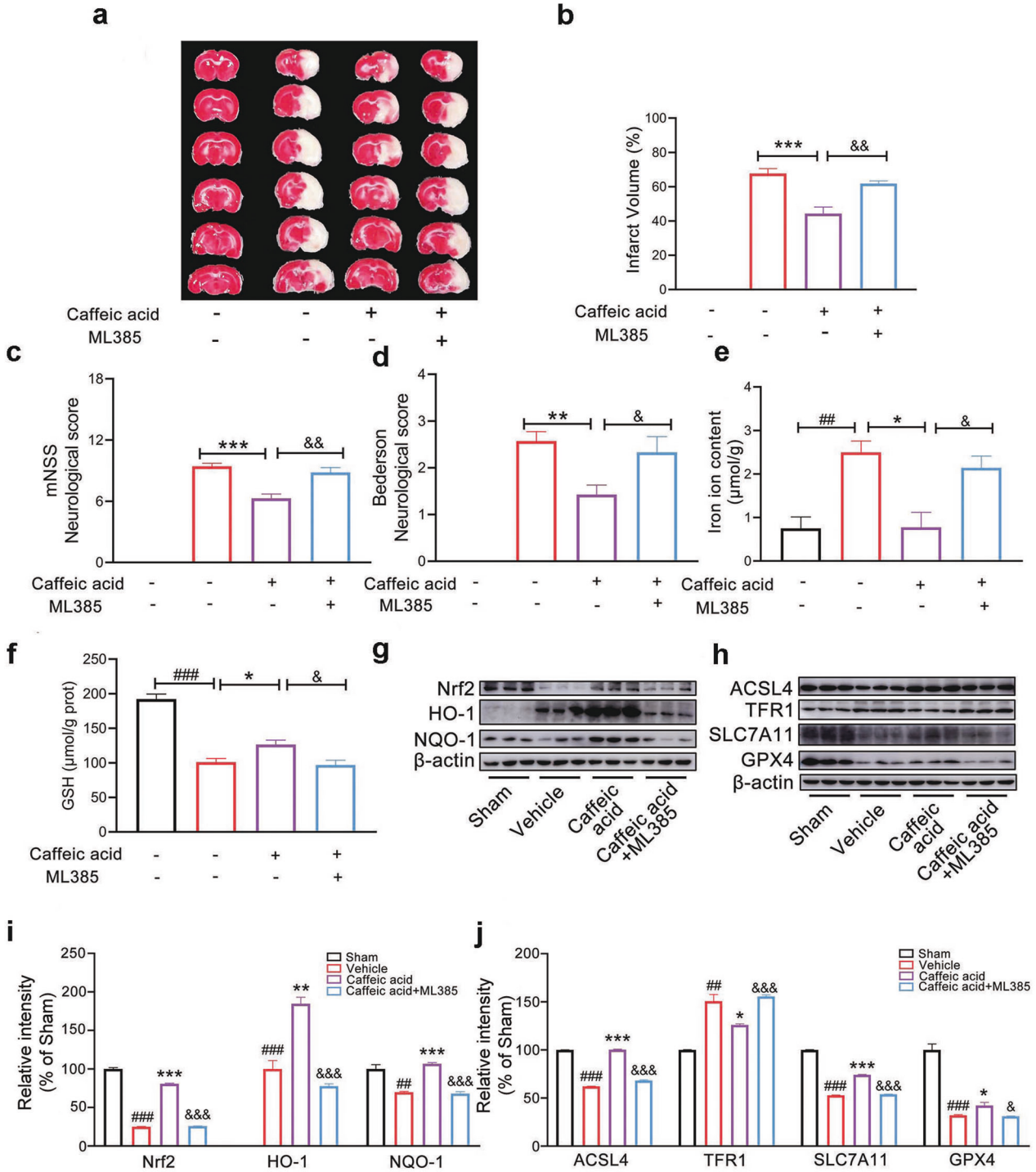

Fig. 8 Caffeic acid reversed ferroptosis via the Nrf2 signaling pathway in vivo. a, **b** Cerebral infarction volume of pMCAO rats. **c** mNSS Neurobehavioural scores of pMCAO rats. **d** Bederson Neurobehavioural scores of pMCAO rats (sham group: $n = 3$, vehicle group: $n = 7$, caffeic acid group: $n = 7$ and ML385 group: $n = 6$). ML385 reversed the protective effect of caffeic acid on iron content (**e**) and GSH content (**f**) in pMCAO rats ($n = 3$). **g**, **i** The effects of ML385 on the expression of Nrf2, HO-1, and NQO-1 ($n = 3$). **h**, **j** The effects of ML385 on the expression of ACSL4, TFR1, SLC7A11, and GPX4 ($n = 3$). Data are shown as the mean ± SEM, $^{\#\#}P < 0.01$, $^{\#\#\#}P < 0.001$ vs. the sham group, $^{*}P < 0.05$, $^{**}P < 0.01$ and $^{***}P < 0.001$ vs. the vehicle group, $^{\&}P < 0.05$, $^{\&\&}P < 0.01$, and $^{\&\&\&}P < 0.001$ vs. the caffeic acid group.

Furthermore, we chose primary cells to confirm the anti-ferroptosis function of caffeic acid in cerebral ischemia. In the OGD/R injury model of primary neurons (Fig. 11a), caffeic acid strongly upregulated the Nrf2 signaling pathway to resist ferroptosis (Fig. 11b–e). In the primary microglia-neuron Transwell cell model (Fig. 11f), LPS-stimulated microglia further led to ferroptosis of neurons after OGD treatment, which was manifested as an increase in the levels of TFR1 and ACSL4 and a decrease in the levels of SLC7A11 and GPX4. Surprisingly, the addition of caffeic acid reversed the inflammatory response of microglia and ferroptosis of neurons in this primary neuro-microglia Transwell cell model (Fig. 11g–j).

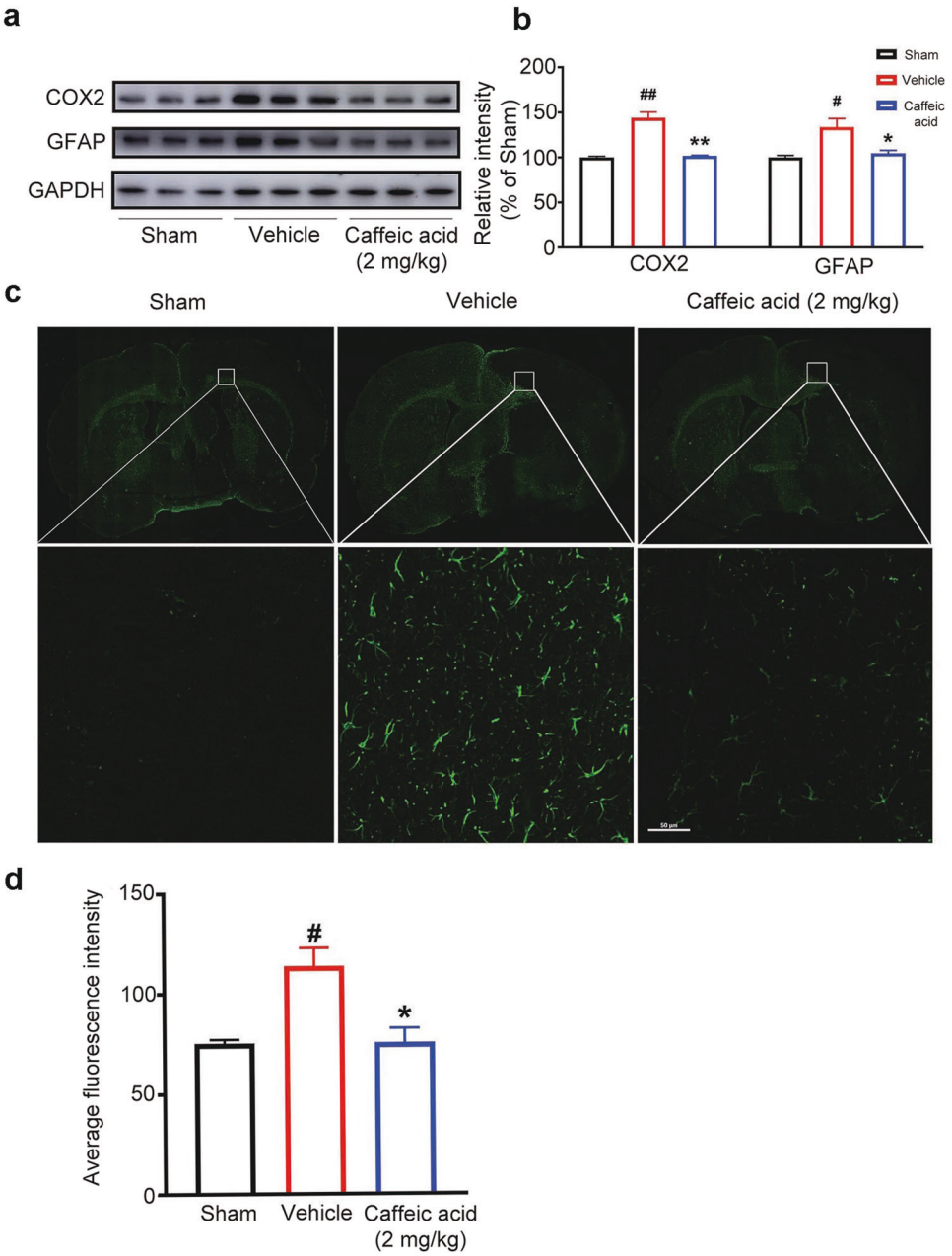

Fig. 9 Caffeic acid exerted anti-inflammatory properties in pMCAO rats. a, **b** The expression of GFAP and COX2 was measured by Western blotting ($n = 3$). **c**, **d** Representative immunofluorescence staining of GFAP and the average fluorescence intensity ($n = 3$). Data are shown as the mean ± SEM, $^{\#}P < 0.05$, $^{\#\#}P < 0.01$ vs. the sham group, $^{*}P < 0.05$ and $^{**}P < 0.01$ vs. the vehicle group.

DISCUSSION

Stroke is an enormous public health problem of growing importance [52]. As the most common type of stroke, ischemic stroke is a disease with high mortality and disability rates [53]. Blood flow is cut off due to the formation of an embolism. This ischemic environment further produces large amounts of ROS in the brain. The presence of ROS causes ferroptosis and inflammation, which further aggravate neuronal damage [54].

Phenolic compounds are a class of compounds isolated from plants that are considered to have the potential to scavenge free radicals due to their stable structure after adsorption of free radicals [55]. Caffeic acid, as a kind of phenolic acid widely existing in nature, has an inherent antioxidant biological function [30]. First, we explored the scavenging ability of caffeic acid on different types of free radicals and found that caffeic acid was much stronger than vitamin C in scavenging DPPH free radicals, hydroxyl free radicals and oxygen free radicals. However, caffeic acid had a weaker scavenging capacity for superoxide anions than vitamin C, which might be due to the strong scavenging ability of caffeic acid for certain types of free radicals. In brain tissue, there are not enough antioxidant defences to clear ROS and other free radicals, so the tissues around the ischemic core are damaged [56]. This free radical scavenging biological function of caffeic acid warrants the further study of its protective effect on ischemic stroke.

In vitro and in vivo studies have shown that caffeic acid not only has antioxidant capacity but also has immunomodulatory, antimicrobial, neuroprotective, antiproliferative and anti-inflammatory activities and has been shown to ameliorate inflammation and oxidative stress in chronic metabolic diseases

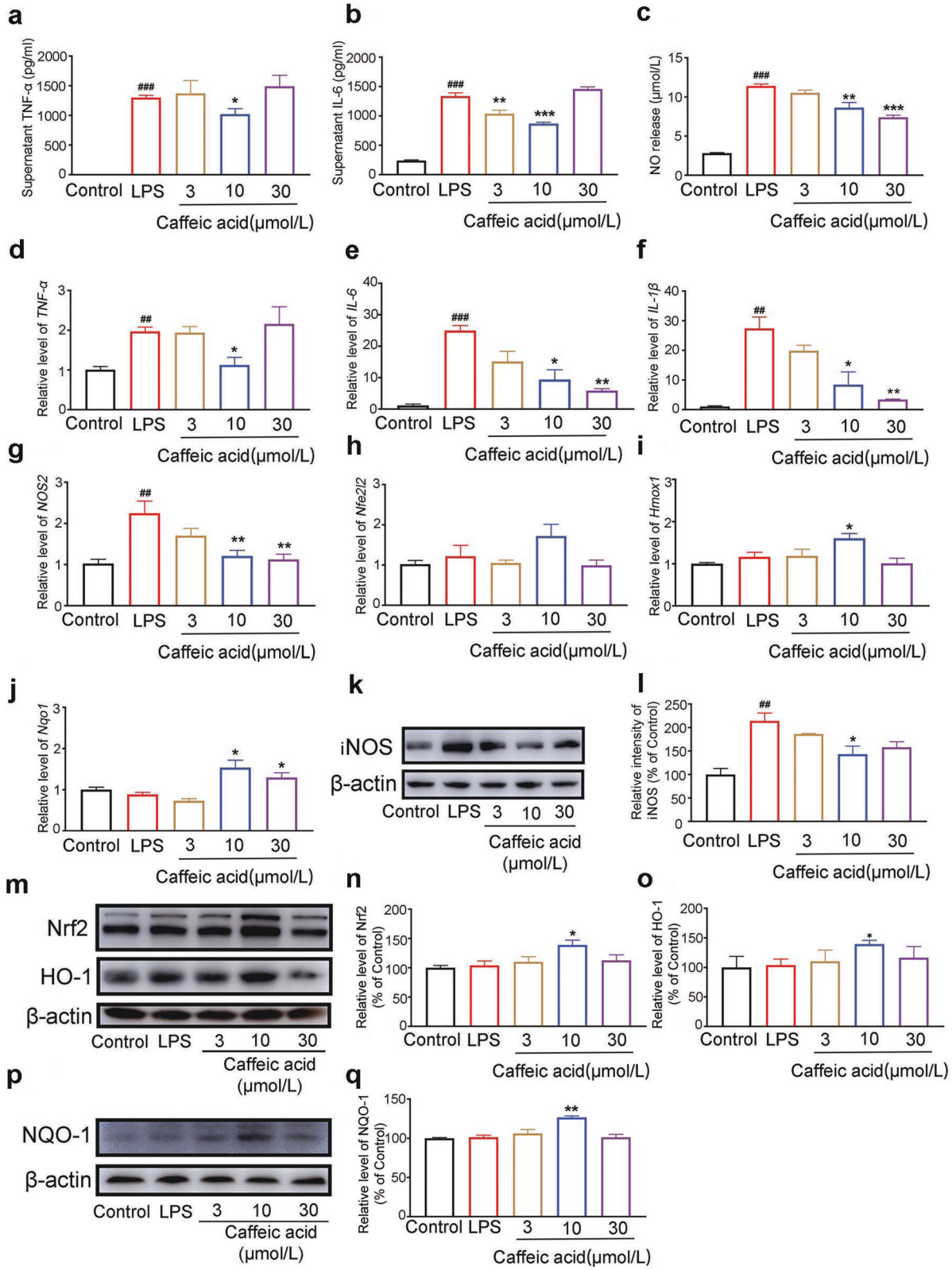

Fig. 10 Caffeic acid suppressed the LPS-induced proinflammatory response in BV2 cells via Nrf2 signaling. The levels of TNF-α (**a**), IL-6 (**b**) and NO (**c**) were detected in the supernatant of LPS-stimulated BV2 cells ($n = 4–5$). Caffeic acid suppressed *TNF-α* (**d**), *IL-6* (**e**), *IL-1β* (**f**) and *NOS2* (**g**) mRNA levels in LPS-stimulated BV2 cells ($n = 3–6$). **h**–**j** The effects of caffeic acid on *Nfe2l2*, *Hmox1* and *Nqo1* mRNA levels were measured by qRT–PCR ($n = 3–6$). **k**, **l** Caffeic acid also suppressed the expression of iNOS in LPS-stimulated BV2 cells ($n = 3$). **m**–**q** The effects of caffeic acid on Nrf2, HO-1 and NQO-1 expression were detected by Western blotting assays ($n = 3$). Data are shown as the mean ± SEM, $^{\#\#}P < 0.01$ and $^{\#\#\#}P < 0.001$ vs. the control group, $^{*}P < 0.05$, $^{**}P < 0.01$ and $^{***}P < 0.001$ vs. the model group.

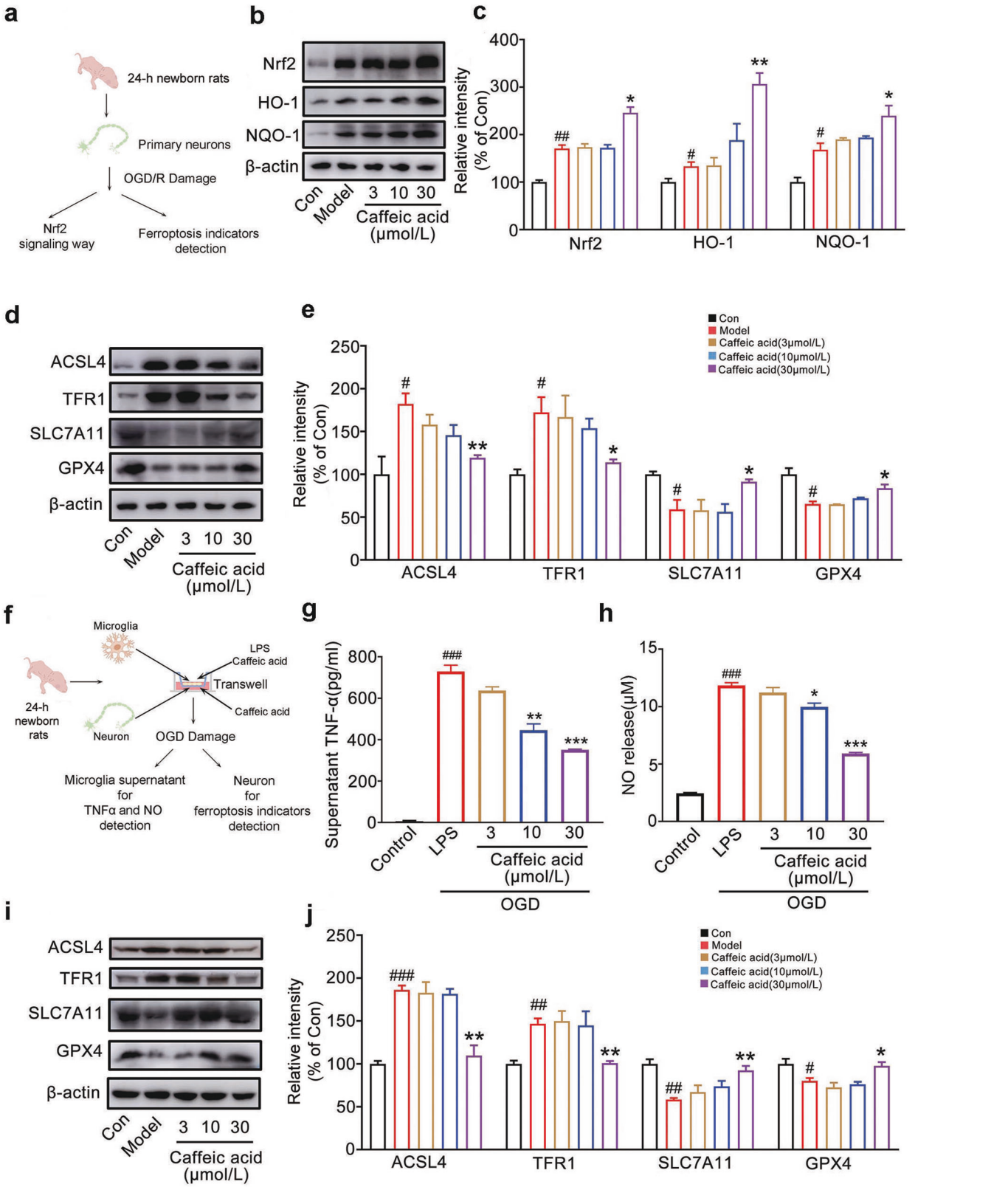

Fig. 11 Caffeic acid inhibited ferroptosis via the Nrf2 signaling pathway in OGD/R primary neurons and a coculture system of microglia and neurons. a Experimental design process of OGD/R damage in primary neurons. **b**, **c** The effects of caffeic acid on Nrf2, HO-1 and NQO-1 protein levels in OGD/R primary neurons ($n = 3$). **d**, **e** The effects of caffeic acid on ACSL4, TFR1, SLC7A11 and GPX4 protein levels in OGD/R primary neurons ($n = 3$). **f** Experimental design process of OGD damage in a coculture system of microglia and neurons. The levels of TNF-α (**g**) and NO (**h**) were detected in the supernatant of LPS-stimulated primary microglia ($n = 3$). **i**, **j** The effects of caffeic acid on ACSL4, TFR1, SLC7A11 and GPX4 protein levels in primary neurons in the coculture system ($n = 3$). $^{\#}P < 0.05$, $^{\#\#}P < 0.01$ and $^{\#\#\#}P < 0.001$ vs. the control group, $^{*}P < 0.05$, $^{**}P < 0.01$ and $^{***}P < 0.001$ vs. the model group.

[57–60]. In our experiment, the protective effect of caffeic acid on brain injury in pMCAO rats was first studied by preadministration. The effect of caffeic acid was preliminarily revealed by the decrease in cerebral infarction volume and the improvement in neurological impairment after 24 h of ischemia. The effect of caffeic acid was further confirmed by postoperative administration and prolonged middle cerebral artery occlusion. Fortuitously, similar improvements in cerebral ischemia were also found. Considering the antioxidant biological function of caffeic acid, oxidative stress in the brain tissue of pMCAO rats was investigated, which was divided into two aspects: oxidative damage and antioxidant capacity. Cerebral ischemia induces the production of ROS and causes an imbalance between generation and elimination, thus destroying lipids, DNA, and proteins and leading to several injuries. Caffeic acid reduced MDA and 8-OHDG levels and improved lipid and DNA oxidative damage. On the other hand, caffeic acid enhanced the antioxidant capacity of brain tissue by increasing GSH levels and GPx activity. Furthermore, we constructed a cellular model of oxygen–glucose deprivation/reoxygenation (OGD/R) injury to expand upon the different conditions of ischemic stroke. Our investigation demonstrated that caffeic acid also played an antioxidant protective role in vitro by reducing ROS levels and increasing antioxidant content and antioxidant enzyme activity after OGD/R.

Nrf2 is considered a cytoprotective factor regulating the expression of genes coding for antioxidant, anti-inflammatory and detoxifying proteins [61]. Nrf2-downstream proteins mitigated the deleterious effects by neutralizing ROS in ischemic stroke [24]. Recent studies have shown that many Nrf2-activating compounds exert excellent protective effects in ischemic stroke models. For example, curcumin, an effective activator of Nrf2, decreased infarct size and improved brain edema in cerebral I/R injury by activating the Nrf2/ARE signal pathway [62]. In this study, caffeic acid-treated brains or cells had a significantly higher level of Nrf2, together with its downstream protein after ischemia stroke. GSK3β, which could regulate Nrf2 [63], was inactivated by phosphorylation of serine. However, p-AKT inhibits GSK3β activity through Ser9 phosphorylation [64]. Our results revealed that caffeic acid upregulated the p-AKT/GSK3β/Nrf2 signaling pathway after cerebral ischemia. GCLC and GCLM, as downstream targets of Nrf2, are the key determinants of GSH synthesis [65]. After MCAO, the levels of GCLC and GCLM were decreased in rat brain tissues, suggesting that the ability to synthesize glutathione was affected. Nrf2 inhibition with ML385 resulted in a drastic reduction in Nrf2 expression levels and abolished the protective effects of caffeic acid, suggesting that the Nrf2 signaling pathway is the key to the protective effect.

A previous study demonstrated that neuronal necrosis and apoptosis play important roles in acute cerebral ischemia [38]. However, targeting neuronal necrosis and apoptosis caused by cerebral ischemia in clinical experiments failed, suggesting that other forms of neuronal death might also play a key role [66, 67]. As a newly discovered type of regulated cell death, ferroptosis is defined as an iron dependent, lipid peroxide-driven form of cell death that is different from other cell death processes [68, 69]. Abnormal accumulation of iron was found in ferroptosis. Transferrin receptor 1 (TFR1), as a key iron transporter on the cell membrane, leads to iron uptake into the cell and enhanced lipid peroxide production. Evidence has shown that TFR1 overexpression also induces selective sensitivity to ferroptosis [70]. Our study showed that caffeic acid reduced iron uptake by reducing TFR1 expression levels. Lipid peroxidation is also a common feature of many disease states and a key trigger of ferroptosis. Our study showed that caffeic acid significantly reduced iron ion and MDA content in vitro and in vivo. Aside from iron ion and lipid peroxidation, low levels of the reducing agent NADPH and the enzyme acyl-CoA synthetase long chain family member 4 (ACSL4), which metabolizes lipid peroxides, are both biomarkers associated with increased sensitivity to ferroptosis [71, 72]. Caffeic acid also reversed the decrease in NADPH and the increase in ACSL4 in the OGD/R damage cell model. However, we found that ACSL4 was reduced in the brain of pMCAO rats compared to the sham group, which was a very thought-provoking finding. A recent study also found that ACSL4 expression was significantly reduced in the tMCAO model before nonreperfusion and increased with subsequent reperfusion time [2], which was consistent with our experimental results in the pMCAO model. The decrease in ACSL4 in the vehicle group may be a biological compensatory effect. In addition, ACSL4 had normal biological functions, and it could catalyze the conversion of long-chain fatty acids to their active form acyl-CoA for both synthesis of cellular lipids and degradation via beta-oxidation [73–75], which may be the main reason for the higher expression of ACSL4 in the sham group. On the other hand, ACSL4 was significantly decreased upon OGD treatment alone but significantly increased in vitro after reoxygenation [2], consistent with our OGD/R cell model. Therefore, we boldly speculated that the change in ACSL4 expression was closely related to whether reperfusion/reoxygenation was performed in vivo and in vitro. In conclusion, the effect of caffeic acid on the level of ACSL4 after cerebral ischemic injury in vivo and in vitro was always consistent with that in the sham and control groups.

GSH, which is a simple tripeptide consisting of glutamate, cysteine, and glycine, enables cells to mount antioxidant defences. Specifically, GSH was used by GPX4 to reduce lipid peroxides to their alcohol form, which is an important measure against ferroptosis. The production of glutathione did not occur without the presence of the cystine/glutamate transporter system xC-/xCT, GCLC, GCLM, GSS and GSR. Due to the existence of these key factors, caffeic acid could improve the level of GSH after ischemia. Interestingly, the transcription of many essential antiferroptotic pathway genes is under the control of Nrf2. Several ferroptosis-inducing agents initiate the ferroptotic cascade via inhibition of GPX4 and the cystine/glutamate transporter system xC-/xCT, both of which are downstream targets of Nrf2 [68]. The addition of ML385 eliminated the inhibitory effect of caffeic acid on ferroptosis in vitro and in vivo, which was reflected in the decrease in GSH levels and the increase in iron ion and MDA levels. Our results suggested that caffeic acid further inhibited ferroptosis after cerebral ischemia through the Nrf2-regulated GSH pathway.

An increasing number of studies have found that the interaction between oxidative stress and inflammation could lead to a vicious cycle that aggravates neural damage [76]. Therefore, compounds with antioxidant and anti-inflammatory activities might be beneficial for stroke treatment. Previous studies indicated that caffeic acid phenethyl ester (CAPE) emerged as a useful bioactive compound due to its potent anti-inflammatory activity [77]. However, fewer studies have focused on the anti-inflammatory activity of caffeic acid. In the present research, the anti-inflammatory activity of caffeic acid was confirmed both in vivo and in vitro. Caffeic acid inhibited the production of inflammatory factors including TNF-α, IL-6 and NO in LPS-stimulated BV2 cells. In addition, caffeic acid also regulated the mRNA expression and protein expression of inflammatory factors such as TNF-α, IL-6 and iNOS. Caffeic acid also exerted anti-inflammatory activity in the brains of pMCAO rats by inhibiting the expression of COX-2 and iNOS and suppressing the activation of astrocytes. Moreover, caffeic acid exhibited anti-inflammatory activity by upregulating the Nrf2 signaling pathway. The microglia of the brain are activated within minutes after ischemic onset and lead to the overproduction of ROS, NO and proinflammatory cytokines such as TNF-α and IL-6, aggravating brain damage [78, 79]. More importantly, overproduction of NO could react with ROS and form peroxynitrite (ONOO-) in BV2 microglia, which is a more toxic product that causes cell damage [80, 81]. As a result, caffeic acid robustly reduced brain damage and ameliorated

neuroinflammation in rats after cerebral ischemia stroke, which was largely due to the anti-neuroinflammatory properties of caffeic acid in microglia via Nrf2 activation. These findings implied that the treatment effect of caffeic acid on ischemic stroke was closely related to its anti-inflammatory activity. Based on the above experiments, we further used the primary neuron OGD/R injury model and primary microglia-neuron coculture system to explore the neuroprotective effect of caffeic acid. Reduced inflammatory responses in primary microglia and reduced ferroptosis in primary neurons were further observed when caffeic acid was added. Together, these results suggested that caffeic acid attenuated neuroinflammation and resisted ferroptosis in ischemic brain injury via the Nrf2 signaling pathway.

Caffeic acid could regulate Nrf2 to play a protective role in cerebral ischemia. In addition, caffeic acid is also an inhibitor of 5-lipoxygenase [82]. We further investigated the relationship between the activity of 5-lipoxygenase in the Nrf2 signaling pathway by in vivo and in vitro experiments. The results showed that the inhibitory effect of caffeic acid on 5-lipoxygenase did not vanish when the Nrf2 inhibitor ML385 was used (Fig. S7a, b). These results suggested that the Nrf2 upregulation effect of caffeic acid was independent of its inhibitory effect on 5-lipoxygenase. Nrf2 plays a critical role in resistance to ferroptosis. Nrf2 target genes are involved in preventing lipid peroxidation and ferroptosis, and the effects are divided into three broad classes: iron/metal metabolism, intermediate metabolism, and GSH synthesis/metabolism [68]. 5-Lipoxygenase catalyses arachidonic acid to form leukotrienes, which are essential for the production of ROS and MDA in various immune and inflammatory diseases. However, different experimental models have investigated the functional role of 5-lipoxygenase in the pathogenesis of ischemia injury, but the conclusions are inconsistent due to cell type and organ specificity [83–86]. In addition, it has been reported that MK-886 is a 5-lipoxygenase inhibitor that prevents myocardial ischemia/reperfusion injury through Nrf2 signaling. Conversely, administration of the Nrf2 inhibitor ML385 greatly abrogated MK-886-mediated cardioprotection [87]. Notably, caffeic acid also acted as a 5-lipoxygenase inhibitor, and its resistance to ferroptosis in cerebral ischemia disappeared when Nrf2 was inhibited in our study. Taken together, our data suggest that caffeic acid exerts its protective effect against cerebral ischemic injury mainly through Nrf2 signaling.

CONCLUSIONS

In conclusion, we demonstrated that caffeic acid was able to reverse the damage caused by cerebral ischemia in vitro and in vivo. Specifically, caffeic acid alleviated cerebral ischemic injury by regulating ferroptosis via the Nrf2 signaling pathway. These data provide new insight into the mechanisms of ferroptosis and the Nrf2 pathway in ischemic stroke. Moreover, our findings extend the pharmacological function of caffeic acid and provide a clear therapeutic implication for ischemia stroke.

ACKNOWLEDGEMENTS

This project was supported by grants from the National Key R&D Program of China (No. 2019YFC1708901), the National Natural Science Foundation of China (No. 82073835), and the CAMS Innovation Fund for Medical Sciences (No. 2021-I2M-1-028 and 2022-I2M-2-002).

AUTHOR CONTRIBUTIONS

XNL: Performing the experiments, Investigation, Methodology, Validation, Formal analysis, Writing the original draft; NYS: Performing the experiments, Investigation, Methodology, Validation, Formal analysis, Writing the original draft; YYK: Performing the experiments, Methodology; NS: Performing the experiments, Methodology; JQL: Performing the experiments, Methodology; JST: Performing the experiments, Methodology; LW: Methodology, Supervision; JLZ: Conceptualization, Funding acquisition, Project administration, Supervision, Validation; YP: Conceptualization, Funding acquisition, Project administration, Supervision, Validation and Writing-review. All authors have read and approved the final manuscript. All data were generated in-house and no paper mill was used. All authors agree to be accountable for all aspects of the work, ensuring its integrity and accuracy.

ADDITIONAL INFORMATION

Supplementary information The online version contains supplementary material available at https://doi.org/10.1038/s41401-023-01177-5.

Competing interests: The authors declare no competing interests.

REFERENCES

1. Owolabi MO, Thrift AG, Mahal A, Ishida M, Martins S, Johnson WD, et al. Primary stroke prevention worldwide: translating evidence into action. Lancet Public Health. 2022;7:e74–e85.
2. Cui Y, Zhang Y, Zhao X, Shao L, Liu G, Sun C, et al. Acsl4 exacerbates ischemic stroke by promoting ferroptosis-induced brain injury and neuroinflammation. Brain Behav Immun. 2021;93:312–21.
3. Cohen JE, Itshayek E, Moskovici S, Gomori JM, Fraifeld S, Eichel R, et al. State-of-the-art reperfusion strategies for acute ischemic stroke. J Clin Neurosci. 2011;18:319–23.
4. Kelmanson IV, Shokhina AG, Kotova DA, Pochechuev MS, Ivanova AD, Kostyuk AI, et al. In vivo dynamics of acidosis and oxidative stress in the acute phase of an ischemic stroke in a rodent model. Redox Biol. 2021;48:102178.
5. Sharpe PC, Mulholland C, Trinick T. Ascorbate and malondialdehyde in stroke patients. Ir J Med Sci. 1994;163:488–91.
6. Domínguez C, Delgado P, Vilches A, Martín-Gallán P, Ribó M, Santamarina E, et al. Oxidative stress after thrombolysis-induced reperfusion in human stroke. Stroke. 2010;41:653–60.
7. Kimura-Ohba S, Yang Y. Oxidative DNA damage mediated by intranuclear mmp activity is associated with neuronal apoptosis in ischemic stroke. Oxid Med Cell Longev. 2016;2016:6927328.
8. Ichikawa H, Wang L, Konishi T. Prevention of cerebral oxidative injury by post-ischemic intravenous administration of shengmai san. Am J Chin Med. 2006;34:591–600.
9. Narne P, Pandey V, Phanithi PB. Role of nitric oxide and hydrogen sulfide in ischemic stroke and the emergent epigenetic underpinnings. Mol Neurobiol. 2019;56:1749–69.
10. Xu J, Wang A, Meng X, Yalkun G, Xu A, Gao Z, et al. Edaravone dexborneol versus edaravone alone for the treatment of acute ischemic stroke: A phase iii, randomized, double-blind, comparative trial. Stroke. 2021;52:772–80.
11. Kobayashi S, Fukuma S, Ikenoue T, Fukuhara S, Kobayashi S. Effect of edaravone on neurological symptoms in real-world patients with acute ischemic stroke. Stroke. 2019;50:1805–11.
12. Chen T, Shi R, Suo Q, Wu S, Liu C, Huang S, et al. Progranulin released from microglial lysosomes reduces neuronal ferroptosis after cerebral ischemia in mice. J Cereb Blood Flow Metab. 2022;43:505–17.
13. Friedmann Angeli JP, Krysko DV, Conrad M. Ferroptosis at the crossroads of cancer-acquired drug resistance and immune evasion. Nat Rev Cancer. 2019;19:405–14.
14. Yang WS, SriRamaratnam R, Welsch ME, Shimada K, Skouta R, Viswanathan VS, et al. Regulation of ferroptotic cancer cell death by GPX4. Cell. 2014;156:317–31.
15. Zhu L, Feng Z, Zhang J, Du L, Meng A. Microrna-27a regulates ferroptosis through slc7a11 to aggravate cerebral ischemia-reperfusion injury. Neurochem Res. 2023;48:1370–81.
16. Selim M. Treatment with the iron chelator, deferoxamine mesylate, alters serum markers of oxidative stress in stroke patients. Transl Stroke Res. 2010;1:35–9.
17. Alim I, Caulfield JT, Chen Y, Swarup V, Geschwind DH, Ivanova E, et al. Selenium drives a transcriptional adaptive program to block ferroptosis and treat stroke. Cell. 2019;177:1262–79.e1225.
18. Kaspar JW, Niture SK, Jaiswal AK. Nrf2:Inrf2 (keap1) signaling in oxidative stress. Free Radic Biol Med. 2009;47:1304–9.
19. Theodore M, Kawai Y, Yang J, Kleshchenko Y, Reddy SP, Villalta F, et al. Multiple nuclear localization signals function in the nuclear import of the transcription factor Nrf2. J Biol Chem. 2008;283:8984–94.
20. Krajka-Kuzniak V, Paluszczak J, Baer-Dubowska W. The Nrf2-are signaling pathway: an update on its regulation and possible role in cancer prevention and treatment. Pharmacol Rep. 2017;69:393–402.
21. Pradeep H, Diya JB, Shashikumar S, Rajanikant GK. Oxidative stress-assassin behind the ischemic stroke. Folia Neuropathol. 2012;50:219–30.

22. Shih AY, Li P, Murphy TH. A small-molecule-inducible Nrf2-mediated antioxidant response provides effective prophylaxis against cerebral ischemia in vivo. J Neurosci. 2005;25:10321–35.
23. Liu L, Vollmer MK, Fernandez VM, Dweik Y, Kim H, Dore S. Korean red ginseng pretreatment protects against long-term sensorimotor deficits after ischemic stroke likely through Nrf2. Front Cell Neurosci. 2018;12:74.
24. Duan J, Cui J, Yang Z, Guo C, Cao J, Xi M, et al. Neuroprotective effect of apelin 13 on ischemic stroke by activating AMPK/GSK-3beta/Nrf2 signaling. J Neuroinflammation. 2019;16:24.
25. Buendia I, Michalska P, Navarro E, Gameiro I, Egea J, León R. Nrf2-are pathway: an emerging target against oxidative stress and neuroinflammation in neurodegenerative diseases. Pharmacol Ther. 2016;157:84–104.
26. Johnson DA, Amirahmadi S, Ward C, Fabry Z, Johnson JA. The absence of the pro-antioxidant transcription factor Nrf2 exacerbates experimental autoimmune encephalomyelitis. Toxicol Sci. 2010;114:237–46.
27. Agyeman AS, Chaerkady R, Shaw PG, Davidson NE, Visvanathan K, Pandey A, et al. Transcriptomic and proteomic profiling of keap1 disrupted and sulforaphane-treated human breast epithelial cells reveals common expression profiles. Breast Cancer Res Treat. 2012;132:175–87.
28. Harada N, Kanayama M, Maruyama A, Yoshida A, Tazumi K, Hosoya T, et al. Nrf2 regulates ferroportin 1-mediated iron efflux and counteracts lipopolysaccharide-induced ferroportin 1 mRNA suppression in macrophages. Arch Biochem Biophys. 2011;508:101–9.
29. Campbell MR, Karaca M, Adamski KN, Chorley BN, Wang X, Bell DA. Novel hematopoietic target genes in the Nrf2-mediated transcriptional pathway. Oxid Med Cell Longev. 2013;2013:120305.
30. Khan FA, Maalik A, Murtaza G. Inhibitory mechanism against oxidative stress of caffeic acid. J Food Drug Anal. 2016;24:695–702.
31. Darendelioglu E. Caffeic acid suppresses HT-29 cell death induced by H_2O_2 via oxidative stress and apoptosis. Bratisl Lek Listy. 2020;121:805–11.
32. Jiang RW, Lau KM, Hon PM, Mak TC, Woo KS, Fung KP. Chemistry and biological activities of caffeic acid derivatives from *Salvia miltiorrhiza*. Curr Med Chem. 2005;12:237–46.
33. Yang L, Tao Y, Luo L, Zhang Y, Wang X, Meng X. Dengzhan xixin injection derived from a traditional Chinese herb erigeron breviscapus ameliorates cerebral ischemia/reperfusion injury in rats via modulation of mitophagy and mitochondrial apoptosis. J Ethnopharmacol. 2022;288:114988.
34. Luo L, Wu S, Chen R, Rao H, Peng W, Su W. The study of neuroprotective effects and underlying mechanism of naoshuantong capsule on ischemia stroke mice. Chin Med. 2020;15:119.
35. Mu X, Xu X, Guo X, Yang P, Du J, Mi N, et al. Identification and characterization of chemical constituents in dengzhan shengmai capsule and their metabolites in rat plasma by ultra-performance liquid chromatography coupled with quadrupole time-of-flight mass spectrometry. J Chromatogr B Anal Technol Biomed Life Sci. 2019;1108:54–64.
36. Zhou Y, Fang SH, Ye YL, Chu LS, Zhang WP, Wang ML, et al. Caffeic acid ameliorates early and delayed brain injuries after focal cerebral ischemia in rats. Acta Pharmacol Sin. 2006;27:1103–10.
37. Adeoye O, Hornung R, Khatri P, Kleindorfer D. Recombinant tissue-type plasminogen activator use for ischemic stroke in the united states: a doubling of treatment rates over the course of 5 years. Stroke. 2011;42:1952–5.
38. Gilgun-Sherki Y, Rosenbaum Z, Melamed E, Offen D. Antioxidant therapy in acute central nervous system injury: current state. Pharmacol Rev. 2002;54:271–84.
39. Tobin MK, Bonds JA, Minshall RD, Pelligrino DA, Testai FD, Lazarov O. Neurogenesis and inflammation after ischemic stroke: What is known and where we go from here. J Cereb Blood Flow Metab. 2014;34:1573–84.
40. Wardlaw JM, Murray V, Berge E, del Zoppo G, Sandercock P, Lindley RL, et al. Recombinant tissue plasminogen activator for acute ischaemic stroke: an updated systematic review and meta-analysis. Lancet. 2012;379:2364–72.
41. Longa EZ, Weinstein PR, Carlson S, Cummins R. Reversible middle cerebral artery occlusion without craniectomy in rats. Stroke. 1989;20:84–91.
42. Lo EH. Experimental models, neurovascular mechanisms and translational issues in stroke research. Br J Pharmacol. 2008;153:S396–405.
43. Engel O, Kolodziej S, Dirnagl U, Prinz V. Modeling stroke in mice - middle cerebral artery occlusion with the filament model. J Vis Exp. 2011;6:2423.
44. Feng H, Hu L, Zhu H, Tao L, Wu L, Zhao Q, et al. Repurposing antimycotic ciclopirox olamine as a promising anti-ischemic stroke agent. Acta Pharm Sin B. 2020;10:434–46.
45. Hu Q, Zuo T, Deng L, Chen S, Yu W, Liu S, et al. caryophyllene suppresses ferroptosis induced by cerebral ischemia reperfusion via activation of the Nrf2/HO-1 signaling pathway in MCAO/R rats. Phytomedicine. 2022;102:154112.
46. Peng Y, Shao-Feng XU, Wang L, Feng YP, Wang XL. Effects of chiral NBP on cerebral infarct volume due to transient focal cerebral ischemia. Chin New Drugs J. 2005;14:420–3.
47. Bederson JB, Pitts LH, Tsuji M, Nishimura MC, Davis RL, Bartkowski H. Rat middle cerebral artery occlusion: evaluation of the model and development of a neurologic examination. Stroke. 1986;17:472–6.
48. Chen J, Li Y, Wang L, Zhang Z, Lu D, Lu M, et al. Therapeutic benefit of intravenous administration of bone marrow stromal cells after cerebral ischemia in rats. Stroke. 2001;32:1005–11.
49. Xue Q, Yan D, Chen X, Li X, Kang R, Klionsky DJ, et al. Copper-dependent autophagic degradation of GPX4 drives ferroptosis. Autophagy. 2023;19:1982–96.
50. Li Y, Feng D, Wang Z, Zhao Y, Sun R, Tian D, et al. Ischemia-induced ACSL4 activation contributes to ferroptosis-mediated tissue injury in intestinal ischemia/reperfusion. Cell Death Differ. 2019;26:2284–99.
51. Zhu G, Wang X, Chen L, Lenahan C, Fu Z, Fang Y, et al. Crosstalk between the oxidative stress and glia cells after stroke: from mechanism to therapies. Front Immunol. 2022;13:852416.
52. Collaborators GBDS. Global, regional, and national burden of stroke and its risk factors, 1990-2019: a systematic analysis for the global burden of disease study 2019. Lancet Neurol. 2021;20:795–820.
53. Xu R, Wang L, Sun L, Dong J. Neuroprotective effect of magnesium supplementation on cerebral ischemic diseases. Life Sci. 2021;272:119257.
54. Cheng Y, Song Y, Chen H, Li Q, Gao Y, Lu G, et al. Ferroptosis mediated by lipid reactive oxygen species: a possible causal link of neuroinflammation to neurological disorders. Oxid Med Cell Longev. 2021;2021:5005136.
55. Kashiwada Y, Nishizawa M, Yamagishi T, Tanaka T, Nonaka G, Cosentino LM, et al. Anti-aids agents, 18. Sodium and potassium salts of caffeic acid tetramers from arnebia euchroma as anti-hiv agents. J Nat Prod. 1995;58:392–400.
56. Allen CL, Bayraktutan U. Oxidative stress and its role in the pathogenesis of ischaemic stroke. Int J Stroke. 2009;4:461–70.
57. Kępa M, Miklasińska-Majdanik M, Wojtyczka RD, Idzik D, Korzeniowski K, Smoleń-Dzirba J, et al. Antimicrobial potential of caffeic acid against staphylococcus aureus clinical strains. Biomed Res Int. 2018;2018:7413504.
58. Khan F, Bamunuarachchi NI, Tabassum N, Kim YM. Caffeic acid and its derivatives: antimicrobial drugs toward microbial pathogens. J Agric Food Chem. 2021;69:2979–3004.
59. Koga M, Nakagawa S, Kato A, Kusumi I. Caffeic acid reduces oxidative stress and microglial activation in the mouse hippocampus. Tissue Cell. 2019;60:14–20.
60. Muhammad Abdul Kadar NN, Ahmad F, Teoh SL, Yahaya MF. Caffeic acid on metabolic syndrome: a review. Molecules. 2021;26:4777.
61. He F, Ru X. Wen T. Nrf2, a transcription factor for stress response and beyond. Int J Mol Sci. 2020;21:4777.
62. Yang C, Zhang X, Fan H, Liu Y. Curcumin upregulates transcription factor Nrf2, HO-1 expression and protects rat brains against focal ischemia. Brain Res. 2009;1282:133–41.
63. Rojo AI, Rada P, Egea J, Rosa AO, López MG, Cuadrado A. Functional interference between glycogen synthase kinase-3 beta and the transcription factor Nrf2 in protection against kainate-induced hippocampal cell death. Mol Cell Neurosci. 2008;39:125–32.
64. Ali T, Kim T, Rehman SU, Khan MS, Amin FU, Khan M, et al. Natural dietary supplementation of anthocyanins via PI3K/Akt/Nrf2/HO-1 pathways mitigate oxidative stress, neurodegeneration, and memory impairment in a mouse model of alzheimer's disease. Mol Neurobiol. 2018;55:6076–93.
65. Lu SC. Glutathione synthesis. Biochim Biophys Acta. 2013;1830:3143–53.
66. Hribljan V, Lisjak D, Petrović DJ, Mitrečić D. Necroptosis is one of the modalities of cell death accompanying ischemic brain stroke: from pathogenesis to therapeutic possibilities. Croat Med J. 2019;60:121–6.
67. Fricker M, Tolkovsky AM, Borutaite V, Coleman M, Brown GC. Neuronal cell death. Physiol Rev. 2018;98:813–80.
68. Dodson M, Castro-Portuguez R, Zhang DD. Nrf2 plays a critical role in mitigating lipid peroxidation and ferroptosis. Redox Biol. 2019;23:101107.
69. Hirschhorn T, Stockwell BR. The development of the concept of ferroptosis. Free Radic Biol Med. 2019;133:130–43.
70. Lu Y, Yang Q, Su Y, Ji Y, Li G, Yang X, et al. Mycn mediates tfrc-dependent ferroptosis and reveals vulnerabilities in neuroblastoma. Cell Death Dis. 2021;12:511.
71. Doll S, Proneth B, Tyurina YY, Panzilius E, Kobayashi S, Ingold I, et al. Acsl4 dictates ferroptosis sensitivity by shaping cellular lipid composition. Nat Chem Biol. 2017;13:91–98.
72. Shimada K, Hayano M, Pagano NC, Stockwell BR. Cell-line selectivity improves the predictive power of pharmacogenomic analyses and helps identify nadph as biomarker for ferroptosis sensitivity. Cell Chem Biol. 2016;23:225–35.
73. Klett EL, Chen S, Yechoor A, Lih FB, Coleman RA. Long-chain acyl-coa synthetase isoforms differ in preferences for eicosanoid species and long-chain fatty acids. J Lipid Res. 2017;58:884–94.
74. Klett EL, Chen S, Edin ML, Li LO, Ilkayeva O, Zeldin DC, et al. Diminished acyl-coa synthetase isoform 4 activity in ins 832/13 cells reduces cellular

epoxyeicosatrienoic acid levels and results in impaired glucose-stimulated insulin secretion. J Biol Chem. 2013;288:21618–29.
75. Kang MJ, Fujino T, Sasano H, Minekura H, Yabuki N, Nagura H, et al. A novel arachidonate-preferring Acyl-Coa synthetase is present in steroidogenic cells of the rat adrenal, ovary, and testis. Proc Natl Acad Sci USA. 1997;94:2880–4.
76. Liao S, Wu J, Liu R, Wang S, Luo J, Yang Y, et al. A novel compound DBZ ameliorates neuroinflammation in LPS-stimulated microglia and ischemic stroke rats: role of AKT(ser473)/GSK3β(ser9)-mediated Nrf2 activation. Redox Biol. 2020;36:101644.
77. da Silveira M, Luz DACCS, da Silva CCS, Prediger RDS, Martins MD, Martins MAT, et al. Propolis: a useful agent on psychiatric and neurological disorders? A focus on cape and pinocembrin components. Med Res Rev. 2021;41:1195–215.
78. Guruswamy R, ElAli A. Complex roles of microglial cells in ischemic stroke pathobiology: new insights and future directions. Int J Mol Sci. 2017;18:496.
79. Taylor RA, Sansing LH. Microglial responses after ischemic stroke and intracerebral hemorrhage. Clin Dev Immunol. 2013;2013:746068.
80. Zhang Z, Lv M, Zhou X, Cui Y. Roles of peripheral immune cells in the recovery of neurological function after ischemic stroke. Front Cell Neurosci. 2022;16:1013905.
81. Kumar A, Chen SH, Kadiiska MB, Hong JS, Zielonka J, Kalyanaraman B, et al. Inducible nitric oxide synthase is key to peroxynitrite-mediated, LPS-induced protein radical formation in murine microglial BV2 cells. Free Radic Biol Med. 2014;73:51–9.
82. Yang JQ, Zhou QX, Liu BZ, He BC. Protection of mouse brain from aluminum-induced damage by caffeic acid. CNS Neurosci Ther. 2008;14:10–6.
83. Adamek A, Jung S, Dienesch C, Laser M, Ertl G, Bauersachs J, et al. Role of 5-lipoxygenase in myocardial ischemia-reperfusion injury in mice. Eur J Pharmacol. 2007;571:51–54.
84. Kitagawa K, Matsumoto M, Hori M. Cerebral ischemia in 5-lipoxygenase knockout mice. Brain Res. 2004;1004:198–202.
85. Patel NS, Cuzzocrea S, Chatterjee PK, Di Paola R, Sautebin L, Britti D, et al. Reduction of renal ischemia-reperfusion injury in 5-lipoxygenase knockout mice and by the 5-lipoxygenase inhibitor zileuton. Mol Pharmacol. 2004;66:220–7.
86. Lisovyy OO, Dosenko VE, Nagibin VS, Tumanovska LV, Korol MO, Surova OV, et al. Cardioprotective effect of 5-lipoxygenase gene (ALOX5) silencing in ischemia-reperfusion. Acta Biochim Pol. 2009;56:687–94.
87. Shi KN, Li PB, Su HX, Gao J, Li HH. MK-886 protects against cardiac ischaemia/reperfusion injury by activating proteasome-keap1-Nrf2 signalling. Redox Biol. 2023;62:102706.